Lawrence Berkeley National Laboratory
Recent Work

Title
OXYGEN-17 NUCLEAR MAGNETIC RESONANCE STUDIES OF THE FIRST HYDRATION SPHERE OF DIAMAGNETIC METAL IONS IN AQUEOUS SOLUTION

Permalink
https://escholarship.org/uc/item/0982j318

Author
Neely, James Watson.

Publication Date
1971-06-01

OXYGEN-17 NUCLEAR MAGNETIC RESONANCE
STUDIES OF THE FIRST HYDRATION SPHERE OF
DIAMAGNETIC METAL IONS IN AQUEOUS SOLUTION

James Watson Neely

(Ph. D. Thesis)

June 1971

AEC Contract No. W-7405-eng-48

Table of Contents
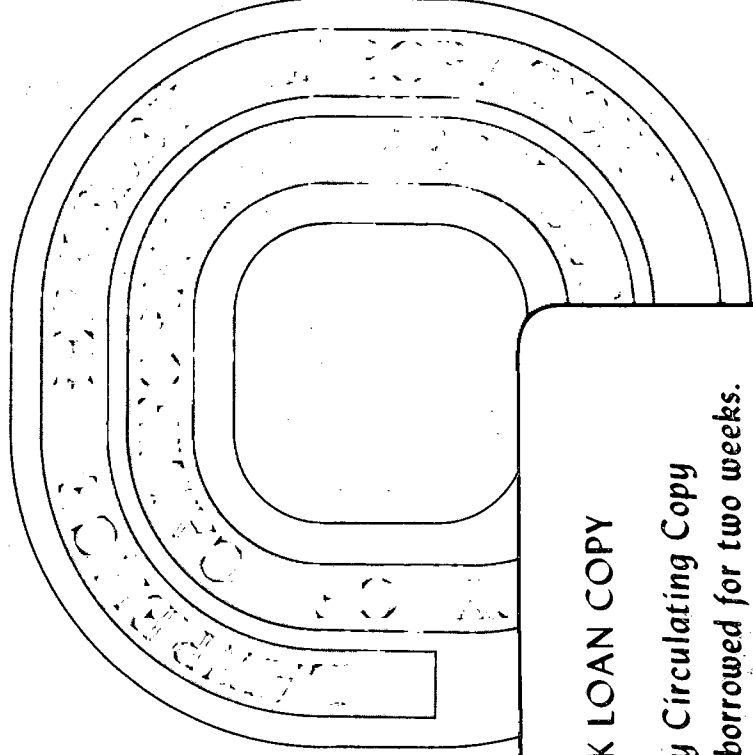
OXYGEN-17 NUCLEAR MAGNETIC RESONANCE STUDIES
OF THE FIRST HYDRATION SPHERE OF DIAMAGNETIC METAL IONS
IN AQUEOUS SOLUTION

James Watson Neely

Inorganic Materials Research Division, Lawrence Radiation Laboratory
Department of Chemistry, University of California,
Berkeley, California

ABSTRACT

The rate of water exchange between hydrated cations and solvent has been measured by observation of the oxygen-17 nmr signal of the waters in the first coordination sphere. Interference from the bulk water resonance was avoided by the addition of sufficient Mn^{2+} to broaden the bulk water signal at least ten times as broad as the bound water signal.

Studies of the bound water linewidth as a function of temperature have resulted in the observation of two distinctly different regions. At higher temperatures the linewidth increases with increasing temperature and is equal to the first order rate constant for exchange of waters with the solvent. The following values for the rate constants at 25°C and the enthalpy and entropy of activation have been measured.

$$Mg^{2+} \quad k = 5.3 \times 10^5 \ sec^{-1}$$
$$\Delta H^{\ddagger} = 10.2 \ kcal/mole$$
$$\Delta S^{\ddagger} = +2 \ eu$$

$$Ga^{3+} \quad k = 7.6 \times 10^2 \ sec^{-1}$$
$$\Delta H^{\ddagger} = 16.5 \ kcal/mole$$
$$\Delta S^{\ddagger} = +10 \ eu$$

$$Be^{2+} \quad k = 2.1 \times 10^3 \ sec^{-1}$$
$$\Delta H^{\ddagger} = 8.3 \ kcal/mole$$
$$\Delta S^{\ddagger} = -15 \ eu$$

$$Al^{3+} \quad k = 16 \ sec^{-1}$$
$$\Delta H^{\ddagger} = 15.6 \ kcal/mole$$
$$\Delta S^{\ddagger} = 0 \ eu$$

At lower temperatures the linewidth decreases with increasing temperature. In this region the linewidth of the bound waters is due to quadrupole interaction of the oxygen-17 in the water molecule modulated by the tumbling of the hydrated cation and the spinning of the waters about the cation-oxygen axis. The magnitude of the relaxation confirms an earlier conclusion that such spinning does occur and is fast enough to cause at least partial averaging of the quadrupole coupling tensor in the water molecule.

Bound oxygen-17 signals have been observed for solutions containing thorium (IV) and indium (III) which are due to oxygen-17 in hydroxide ions contained in hydrolysis products in solution. Exchange parameters for these oxygens have been measured to be:

$$In \ (III) \quad k_{25^o} = 1.7 \times 10^3 \ sec^{-1}$$
$$\Delta H^{\ddagger} = 13 \ kcal/mole$$
$$\Delta S^{\ddagger} = 6 \ eu$$

$$Th \ (IV) \quad k_{25^o} = 7 \times 10^4 \ sec^{-1}$$
$$\Delta H^{\ddagger} = 23 \pm 5 \ kcal/mole$$
$$\Delta S^{\ddagger} = 40 \pm 15 \ eu$$

A general theory is derived for the rate of water exchange based on a simple electrostatic model. The presently available data are shown to be remarkably consistent with the predictions of this model.

No bound water resonance could be observed using the present technique for solutions containing UO_2^{2+}, Tl^{3+}, Sc^{3+} and Zn^{2+}. For these ions only lower limits could be set for the rate of water exchange.

I. INTRODUCTION

Measurement of the rate of water exchange between the first hydration sphere of metal ions and the solvent has been a subject of interest for many years.[1a] Many of the techniques developed to measure fast reactions in solution such as temperature jump and sound absorption cannot measure the water-water exchange reaction because no net chemical change takes place. The technique of isotopic dilution developed by Taube has been useful in instances of very slow exchange such as Cr^{3+} [1b,c] and Rh^{3+} [2]. For more rapidly exchanging systems nuclear magnetic resonance has proven to be the most widely applied method. Broadening of the bulk water nmr resonance of oxygen-17 by paramagnetic metal ions as a function of temperature has yielded much information about the rate of water exchange from these ions.[3]

The use of the nmr technique to determine the rate of exchange from diamagnetic cations has proven to be more difficult experimentally. Diamagnetic metal ions have very little effect on the bulk water linewidth[4] and the bound waters have very little chemical shift relative to the bulk waters. It is necessary to separate the two signals from the two different environments in order to derive information concerning the bound waters.

The bulk waters have been shifted relative to the bound waters by the addition of paramagnetic metal ions such as Co^{2+} or Dy^{3+}.[5] The bulk waters can interact very strongly with these rapidly exchanging ions by exchanging into and out of the first coordination sphere causing a large average chemical shift of the bulk water resonance. The bound waters about a more slowly exchanging ion cannot get into the first coordination sphere of the paramagnetic metal ion and thus

experience a much smaller chemical shift. The linewidth of the bound water resonance can give information about the rate of exchange with the solvent. This method has been used for Al^{3+} and Ga^{3+}.[6a,b] The technique has proven to be useful for average lifetimes in the first coordination sphere of no less than 10^{-2} sec.

Proton magnetic resonance has proven to be quite valuable in coordination number determinations for many ions[7] and in some cases kinetic parameters have been derived as well.[8] However, it is not usually known if the entire water molecule is exchanging or just the protons. Also the extremely low temperatures necessary to separate the bound from bulk proton signals has required mixed solvents such as water-acetone or water-methanol. The possibility of large solvent effects and the large interval of extrapolation to room temperature makes more direct determinations desirable.

The present study has taken a different approach to the problem of separating the bound from the bulk water signal. For the same reason that Co^{2+} shifts only the bulk waters, a paramagnetic ion which produces rapid transverse relaxation of the oxygen-17 nuclei of the bulk waters such as Mn^{2+} would not be expected to relax appreciably the waters in the first coordination sphere of a more slowly exchanging cation. If the bulk waters could be relaxed rapidly enough, the amplitude of their resonance signal would become negligible compared to that of the more slowly relaxing bound waters. Under such conditions the bound water signal could be observed independently of the bulk water signal.

In many cases the linewidth of the bound water signal can yield information about the average lifetime of a water molecule in the environment of a diamagnetic cation. The linewidth of the nmr signal

is equal to the rate at which the precessing nuclei lose phase coherence of the component of magnetization in a plane perpendicular to the external magnetic field. In solutions containing paramagnetic ions the bulk waters have the phase of the perpendicular magnetization randomized very rapidly due to interactions with paramagnetic ions.

Chemical exchange between the bulk waters and the first hydration sphere of the diamagnetic cations will result in the replacement of a bound oxygen-17 possessing a degree of phase coherency with a water from the bulk which will possess a phase of random orientation relative to other bound water oxygen-17 nuclei. Both quadrupole relaxation within the first coordination sphere and chemical exchange with the rapidly relaxing bulk waters will be important mechanisms for the transverse relaxation of bound waters.

The trend with temperature for the two relaxation mechanisms is in opposite directions. At higher temperatures the exchange introduced relaxation dominates and the transverse relaxation time becomes equal to the mean lifetime of a water molecule in the bound environment. The linewidth of the bound water resonance is the reciprocal of the relaxation time which, under these conditions, becomes equal to the first order reaction rate constant for chemical exchange from each site on the bound cation. At sufficiently low temperatures the exchange will become so slow that relaxation is controlled by the quadrupole coupling interactions in the bound environment.

II. THEORY

A phenomenological description of the properties of nuclei in the liquid state in an external magnetic field is provided by the Bloch equations.[9] Under conditions of slow passage and lack of saturation the time independent resonance signal for the absorption mode has been shown to be:[10]

$$S = \sum_{n = -\infty}^{\infty} \frac{2n}{\beta} \frac{J_n^2(\beta) \, |\gamma| \, H_1 M_o T_2}{1 + T_2^2(\Delta\omega \pm n\omega_M)^2} \qquad (1)$$

and $\beta = \dfrac{\gamma H_M}{\omega_M}$ and $\Delta\omega = \omega_o - \omega$ where H_M is the amplitude in gauss of the audio modulation field, ω_M is the frequency of the audio modulation field in Hz, γ is the magnetogyric ratio of the nucleus, H_1 is one half the amplitude in gauss of the radio frequency field, ω_o is the precessional frequency of the nucleus, $J_n(\beta)$ is the Bessel function of the first kind, T_2 is the transverse relaxation time of the nucleus and M_o is the equilibrium value of the magnetization.

Under conditions where

$$\omega_M T_1, \ \omega_M T_2 \gg 1 \qquad (2)$$

Eq. 1 gives sidebands of opposite sign symmetrically displaced about $\omega_o = \omega$ with the center band amplitude zero. Large linewidths make condition (2) difficult or impossible to fulfill. For this reason most experiments in this work were run under the opposite conditions

$$\omega_M T_1, \ \omega_M T_2 \ll 1. \qquad (3)$$

Under these conditions the signal observed is the derivative of the absorption signal.[11]

It is of interest to show mathematically that this result is in fact predicted by Eq. 1. Equation 1 can be rewritten

$$S = \frac{- 8 \, |\gamma| \, H_1 \, T_2^3 \, M_o \, \omega_M \, \Delta\omega}{\beta} \sum_{n=0}^{\infty} \frac{n^2 \, J_n^2 \, (\beta)}{B + A} \qquad (4)$$

$$A = n^2 \, \omega_M^2 \, T_2^2 \, [n^2 \, \omega_M^2 \, T_2^2 + 2(1 - \Delta\omega^2 \, T_2^2)]$$

$$B = [1 + \Delta\omega^2 \, T_2^2]^2 .$$

Since

$$\lim_{n\to\infty} n^2 \, J_n^2(\beta) = \frac{n}{2\pi} \left(\frac{e\beta}{2n} \right)^{2n} \to 0 \qquad {}^{12} \qquad (5)$$

Eq. 4 will reduce to

$$S = \frac{- 8 \, |\gamma| \, H_1 \, T_2^3 \, M_o \, \omega_M \, \Delta\omega}{\beta \, [1 + \Delta\omega^2 \, T_2^2]^2} \sum_{n=0}^{\infty} n^2 J_n^2(\beta) \qquad (6)$$

if during the summation to higher n the term A remains small compared to B until $n^2 J_n^2(\beta)$ becomes small enough that higher order terms can be neglected. It can be shown by numerical evaluation of the series $\sum_{n=0}^{\infty} n^2 J_n^2(\beta)$ that the first $\beta + 1$ terms of the series equal about 95% of the limiting value of the summation which is shown in Appendix 1 to be $\frac{\beta^2}{4}$. The most restrictive case for term A remaining small compared to term B is when $\Delta\omega = 0$. We are left with the condition that

$$n^2 \, \omega_M^2 \, T_2^2 \, [n^2 \, \omega_M^2 \, T_2^2 + 2] \ll 1. \qquad (7)$$

Each term in the sum must individually be much less than 1 so that

$$(n^2 \, \omega_M^2 \, T_2^2)^2 \ll 1 \qquad (8a)$$

$$2n^2 \, \omega_M^2 \, T_2^2 \ll 1. \qquad (8b)$$

Condition (8a) implies that $(n^2 \omega_M^2 \, T_2^2)^2 \ll 2 \, n^2 \, \omega_M^2 \, T_2^2$. Therefore condition (8b) is sufficient. Setting $n = \beta + 1$ in (8b) we get

$$\gamma \, H_M \, T_2 + \omega_M \, T_2 \ll \frac{1}{\sqrt{2}} . \qquad (9)$$

When condition (9) holds, we get for a final form for Eq. 4

$$\text{Signal} = \frac{- 2 \, \gamma^2 \, H_1 \, H_M \, T_2^3 \, M_o \, \Delta\omega}{[1 + \Delta\omega^2 \, T_2^2]^2} \qquad (10)$$

which is the familiar equation for the derivative of an adsorption signal. It is independent of ω_M and directly proportional to H_M subject to the condition (9). Condition (9) is the well known restriction that both the modulation amplitude and frequency must be much smaller than the linewidth.

Zeros in the derivative of Eq. 10 occur at $\Delta\omega = \frac{\pm 1}{\sqrt{3}} \frac{1}{T_2}$, implying that the measurement of the peak to peak separation of the derivative signal is a measure of the transverse relaxation time of the nucleus according to Eq. 11.

$$\frac{1}{T_2} = \frac{\sqrt{3}}{2} \, \Delta\omega_d \qquad (11)$$

where $\Delta\omega_d$ is the peak to peak separation of the derivative signal.

For the data reported in this study a more accurate method was employed for the computation of $\frac{1}{T_2}$ from the derivative signals. A nonlinear least-square best fit computer program was written with five adjustable parameters assuming a derivative absorption signal. Lacking on-line capability, approximately 60 points were selected from the graphical output of the nmr apparatus for the data set of the program. For instances where two overlapping derivative lines were observed, an eight parameter fit was employed and proportionately more data points

were selected. The estimated error limits for using Eq. 11 were
generally about ± 10%, whereas the above procedure resulted in standard
deviations of the order of ± 2%.

The theoretical interpretation of the physical effects causing the
transverse relaxation of the nucleus is of primary concern. McConnell[13]
modified the Bloch equations[9] to include the possibility of chemical
exchange. Swift and Connick[3] provided a general equation for the ex-
change of nuclei between different environments where the population of
one environment was much greater than that of any other environment.
This condition is not met for the present experiments since concentrated
samples are necessary to make the bound water signal intense enough to
be observable.

Using the notation of Swift and Connick, the steady state Bloch
equations for a two site system become

$$- A\, G_a + \frac{G_b}{\tau_{ba}} = i\, \omega_i\, M_o^a$$

$$- B\, G_b + \frac{G_a}{\tau_{ab}} = i\, \omega_i\, M_o^b \tag{12}$$

where τ_{ab} is the lifetime for the exchange of the nucleus from the _a_
environment to the _b_ environment, G_a is the complex sum of the in and
out of phase components of magnetization of the _a_ environment in the
plane perpendicular to H_o, and

$$A = \frac{1}{T_{2a}} + \frac{1}{\tau_{ab}} - i\, \Delta\omega_a \quad .$$

Solving the simultaneous equations gives

$$G_a = \frac{- i\, \omega_i \left[B\, M_o^a + \frac{M_o^b}{\tau_{ab}} \right]}{AB - \frac{1}{\tau_{ab}\tau_{ba}}} \quad . \tag{13}$$

A similar equation can be written for G_b with _a_'s and _b_'s reversed. No
terms in this equation are a priori negligibly small.

Clearing the denominator of imaginary terms and retaining only the
purely imaginary terms (the out of phase component of G_a or V_a) yields,
as Eq. 14:

$$v_a = \frac{\omega_i M_o^a C + \omega_i M_o^b \left[\dfrac{\dfrac{1}{\tau_{ba} T_{2b}} + \dfrac{1}{\tau_{ba}^2}}{\left(\dfrac{1}{T_{2b}} + \dfrac{1}{\tau_{ba}}\right)^2 + \Delta\omega_b^2} \right] C + \omega_i M_o^b \left[\dfrac{\Delta\omega_b}{\tau_{ba}\left(\dfrac{1}{T_{2b}} + \dfrac{1}{\tau_{ba}}\right)^2 + \Delta\omega_b^2} \right] D}{C^2 + D^2}$$

where

$$C = \frac{1}{T_{2a}} + \frac{1}{\tau_{ab}} - \frac{\dfrac{1}{T_{2b}} + \dfrac{1}{\tau_{ba}}}{\tau_{ab}\tau_{ba} \left[\left(\dfrac{1}{T_{2b}} + \dfrac{1}{\tau_{ba}}\right)^2 + \Delta\omega_b^2 \right]} \tag{14}$$

$$D = \Delta\omega_a + \frac{\Delta\omega_b}{\tau_{ab}\tau_{ba} \left[\left(\dfrac{1}{T_{2b}} + \dfrac{1}{\tau_{ba}}\right)^2 + \Delta\omega_b^2 \right]}$$

Again a similar expression for v_b can be written with _a_'s and _b_'s
reversed. The total observed signal will be the sum $v = v_a + v_b$.

The _a_ environment will refer to the bound environment and _b_ to the
bulk. The physical conditions are arranged for this work such that

$$\frac{1}{T_{2b}} \gg \frac{1}{T_{2a}}, \frac{1}{\tau_{ab}}, \frac{1}{\tau_{ba}}, |\Delta\omega_b| \quad . \tag{15}$$

Under these conditions* it can be seen from Eq. 14 and the similar

---

*The general condition under which Eq. 16 will be true is:

$$\frac{1}{T_{2b}} + |\Delta\omega_b| \gg \frac{1}{T_{2a}}, \frac{1}{\tau_{ab}}, \frac{1}{\tau_{ba}}$$

expression for v_b that:

$$v = v_a = \frac{\omega_i \, M_o \, a \left(\frac{1}{T_{2a}} + \frac{1}{\tau_{ab}}\right)}{\left(\frac{1}{T_{2a}} + \frac{1}{\tau_{ab}}\right)^2 + \Delta\omega_a^2} \quad . \tag{16}$$

This is the familiar expression for a Lorenzian lineshape with half width at half height

$$\frac{1}{T_2} = \frac{1}{T_{2a}} + \frac{1}{\tau_{ab}} \quad . \tag{17}$$

As will be discussed later the physical source of the $\frac{1}{T_{2a}}$ term is quadrupole coupling interrupted by molecular tumbling according to the following equation:[14]

$$\frac{1}{T_{2a}} = \frac{3}{40} \, \frac{2I + 3}{I^2(2I - 1)} \, \left(1 + \frac{\xi^2}{3}\right) \left(\frac{eqQ}{\hbar}\right)^2 \, \tau_r \tag{18}$$

where I is the nuclear spin quantum number, Q is the quadrupole moment of the oxygen-17 nucleus, eq is the largest component of the tensor describing the electric field gradient of the water molecule at the oxygen-17 nucleus, ξ is the asymmetry parameter which describes the deviation of the electric field gradient from axial symmetry and τ_r is the tumbling time of the water molecule given by[15]

$$\tau_r = \frac{4\pi a^3 \eta}{3kT} \tag{19}$$

η is the viscosity in poise of the solution, and a is the radius of the tumbling species which will be taken as the sum of the ionic radius of the metal ion, the ionic radius of oxygen and the Van der Waals radius of oxygen. The assumptions invoked in Eq. 18 and 19 will be considered later.

III. EXPERIMENTAL

A. Sample Preparation

Solutions of Mg^{2+}, Zn^{2+}, Th^{4+}, In^{3+}, UO_2^{2+}, Al^{3+} and Ga^{3+} in 20% oxygen-17 enriched water with natural abundance deuterium were prepared from the reagent grade perchlorate salts unless noted. Except when anhydrous salts were available, all materials were dried, then heated to 100°C under vacuum until less than a few microns of vapor pressure of water could be measured over the salts. Weighed portions were then dissolved in water and eluted from a cation exchange resin. The eluted perchloric acid was titrated with standard base giving the equivalents of metal ion present. The difference between the molecular weight calculated and that of the anhydrous salt was assigned to remaining waters of hydration.

Samples of Tl^{3+} and Sc^{3+} were prepared from the anhydrous chloride salts mixed in appropriate molar amounts with anhydrous silver perchlorate in oxygen-17 enriched water. The solution was separated from the AgCl precipitate by centrifugation and decantation. An aqueous solution of Be^{2+} was prepared directly from the anhydrous chloride salt since chloride ion is known to complex Be^{2+} to a very limited extent.

Perchloric acid was not added to any solution when first prepared to avoid isotopic dilution of the enriched water. Where hydrolysis was suspected, acid was added after initial measurements and subsequent data were compared with the initial data. The exception to this was Tl^{3+} which, because of its strong hydrolysis, required 2M acid in order to obtain an adequate concentration of Tl^{3+} in solution.

B. Experimental Conditions

Experiments were conducted using a Varian Associates Model V4311 fixed frequency unit operated at 8.134 MHz. A Princeton Applied Research model HR-8 lock-in amplifier was used to provide phase sensitive detection and the reference signal for the audio modulation field. The reference signal was amplified and fed into the modulation coils in the probe. A modulation frequency in the range of ca. 50-800 cps was used routinely. The amplitude of the audio modulation was adjusted to be as large as possible for each linewidth, with care being taken to avoid modulation broadening. The audio phase was adjusted by selecting the phase which gave maximum intensity for the derivative signal.

Signal averaging was accomplished using a Varian Associates Model C1024 time averaging computer. The ramp output of the computer was fed directly into the sweep input of the Varian Associates Model (V2100) magnet power supply in order to scan the magnetic field.

Leakage detection was employed for the r.f. field at power settings of 0.5 to ca. 1.0 watt. At these power levels the stability of the leakage became a major problem. The positioning of the receiver coil was critical in the attainment of maximum leakage stability. Because of the signal to noise difficulties, a large filling factor is a necessity. The largest practical filling factor is obtained by placing the receiver coil on the outside of the sample tube. Unfortunately, the sample tube could not be fastened securely enough to eliminate vibrations caused by the flow of the temperature regulating gas past the sample. Greatest leakage stability with least loss of filling factor was gained by attaching the receiver coil to the inside

of the dewared insert. Only the glass of the sample tube and the annular space required for the flow of temperature regulating gas separated the receiver coil and the sample.

Temperature control was maintained by flowing heated or cooled dry nitrogen past the sample which was placed in a dewared insert inside the probe. The temperature was measured to 0.1 deg. with a copper-constantin thermocouple immediately outside the sample tube and regulated to ± 0.2 deg.

The observation of exceptionally broad solution nmr signals has been made possible through the use of signal averaging and large 13 mm thin walled pyrex sample tubes. Bound water signals as broad as 10^5 Hz have been observed and bulkwater lines as wide as 2×10^6 Hz have been detected. The limitation with this experimental method comes not from the difficulty of observation of wide lines but with the efficiency with which the bulk water ^{17}O can be relaxed. Manganous ion is the most efficient means known of relaxing oxygen-17 in water solutions. However Mn^{2+} cannot relax waters at a rate any greater than the rate at which water enters its first coordination sphere. Ions which exchange nearly as fast or faster than Mn^{2+} become experimentally impossible since the bulk water relaxation rate must be an order of magnitude greater than the exchange rate of the ion in question.

IV. RESULTS AND DISCUSSION

A. Magnesium Ion

The linewidth as a function of temperature of the waters in the first coordination sphere of magnesium ion is shown in Fig. 1. The slope and linearity of the data indicate from Eq. (17) that for the temperature range covered $\frac{1}{\tau_{ab}} \gg \frac{1}{T_{2a}}$ and $\frac{1}{T_2} = \frac{1}{\tau_{ab}} = k$. The line-width of the bound water signal is equal to k, the first order reaction rate constant for water exchange from each exchanging site on the Mg^{2+} ion. The apparent first-order reaction rate of the reaction

$$[Mg(H_2O)_6]^{2+} + H_2O^* \rightleftharpoons [Mg(H_2O)_5 H_2O^*]^{2+} + H_2O$$
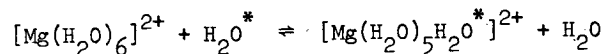
is defined by

$$\text{rate} = 6 k [Mg(H_2O)_6^{2+}]$$

where the coordination number has been taken as six.[16,17,7] The value of k is found to be 5.3×10^5 sec^{-1} at 25°C with an enthalpy and entropy of activation of 10.2 kcal/mole and 2 eu, respectively.

Approximate values of the rate constant for exchange of water molecules from the first coordination sphere of Mg^{2+} ion have been determined previously by various methods. Sonic relaxation and temperature-jump techniques[18-21] are incapable of measuring reactions where no net chemical change takes place, such as water exchange. However, an estimate of the water exchange rate can be obtained by measuring the rate at which a water molecule is replaced by some other ligand in the first coordination sphere, if it is assumed that the rate is primarily controlled by the difficulty of removing the water. The first-order rate constant for the entry of various divalent anions
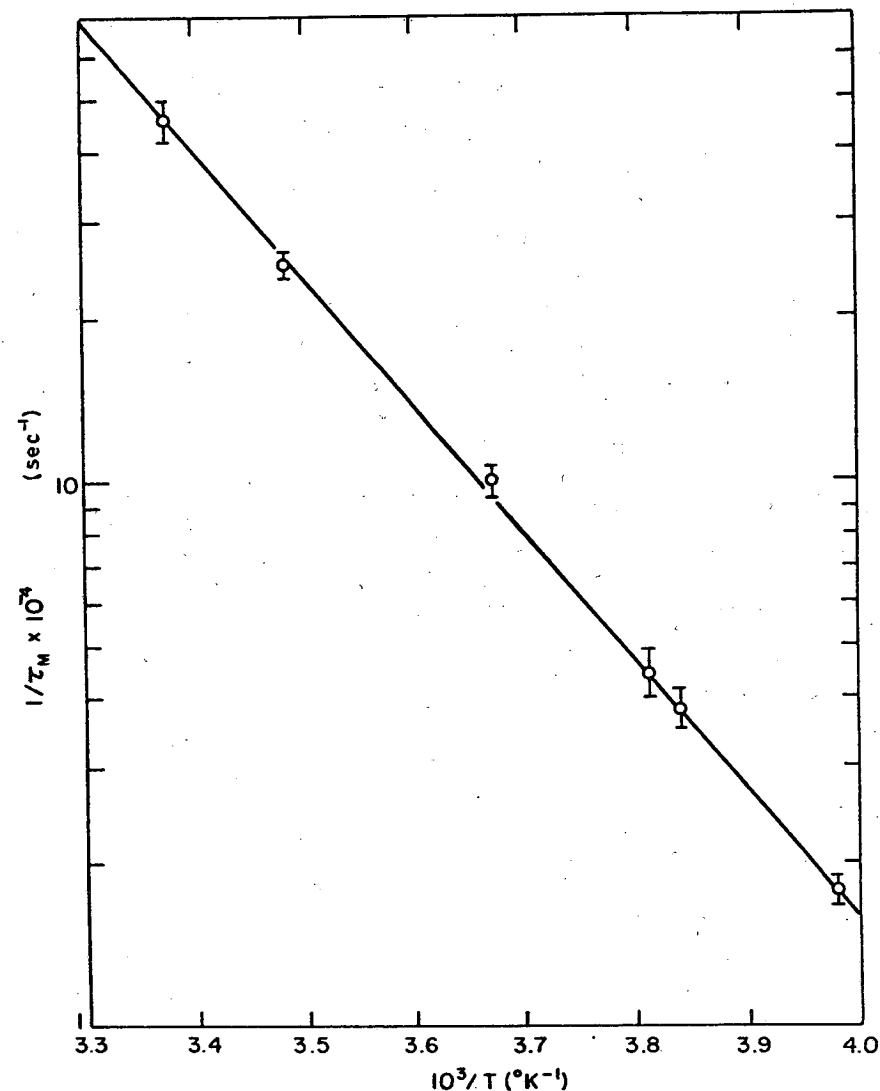
XBL 6912-6685

Fig. 1 Rate of water exchange versus reciprocal of absolute temperature. Composition of solution was 1.30 gm of H_2O enriched to 20% in oxygen-17 (48.7% $H_2^{18}O$), 1.00 gm of $Mg(ClO_4)_2$ (anhydrous), and 0.30 gm of $Mn(ClO_4)_2 \cdot 6H_2O$.

into the first coordination sphere of Mg^{2+} from the second at room
temperature has been measured to be 1×10^5 sec^{-1}.[18] Proton magnetic
resonance techniques are capable of measuring the rate of exchange
directly, but the resonance of the bound protons is resolved from that
of the bulk protons only at temperatures below $-60°$. Rate data have
been obtained only for mixed water-acetone solvents which give an
extrapolated room temperature k of ca. $4-6 \times 10^6$ sec^{-1}.[8] Possible
solvent effects and the large interval of extrapolation to room tempera-
ture make a direct comparison with the present results dubious.

The magnitude of the difference between the present result and
the sound absorption and temperature-jump data is not surprising.
Differences of the same relative size have been noted previously for
transition metal ions.[3] The rate constant for water exchange would be
expected to be $4/3$ that of the rate constant for a ligand entering the
first coordination sphere if it is assumed that only molecules on the
faces of a first sphere octahedron of waters can enter a vacated site.[3]
The fact that the observed water rate is much greater than $4/3$ the
ligand rate may be an indication of the extent to which water is
electrostatically and/or sterically favored over the other ligands
studied in competing for a vacated coordination site.

The possibility of the paramagnetic metal ion (Mn^{2+}) interacting
directly with the first coordinate sphere waters of magnesium ion was
investigated experimentally. The amount of manganese present was varied
from half to four times the concentration of the experimental sample
with no measureable change in the rate of relaxation of the waters
bound to magnesium.

B. Beryllium Ion

The results of a temperature study from -18 to $+90°C$ for an
aqueous solution of Be^{2+} ions is shown in Fig. 2. In this case the
conditions are such that both regions predicted by Eq. 17 are encoun-
tered over the temperature range covered. The data can be seen to be
the sum of two lines labeled $\frac{1}{T_{2a}}$ and $\frac{1}{\tau_{ab}}$. The apparent first-order
reaction rate constant from the $\frac{1}{\tau_{ab}}$ line extrapolated to $25°C$ is
2.1×10^3 sec^{-1} in good agreement with an earlier reported value.[6a] An
enthalpy and entropy of activation of $\Delta H^{\ddagger} = 8.3$ kcal/mole and $\Delta S^{\ddagger} =$
-15 eu were calculated from the $\frac{1}{\tau_{ab}}$ line.

The rate of sulfate ions entering the first coordination sphere
of Be^{2+} ion has been measured at $25°C$ by sound absorption techniques to
be 10^{+2} sec^{-1}.[18] As was noted to be the case for Mg^{2+}, the water
exchange rate is significantly faster than the rate of sulfate entering
the first coordination sphere.

In the low temperature region the temperature dependence of the
linewidth reverses and the relaxation rate becomes dominated by the
relaxation taking place within the bound environment. The quadrupole
interaction interrupted by molecular tumbling according to Eq. 18 is
responsible for the relaxation of oxygen-17 in pure water.[22] Since
the tumbling time of waters in the first coordination sphere of a metal
ion is much greater than that of pure water, the quadrupolar relaxation
mechanism should be even greater for bound waters. Equation 19 predicts
an $\frac{\eta}{T}$ temperature dependence for this region. Figure 3 shows an
experimental plot of $\frac{\eta}{T}$ versus $\frac{10^3}{T}$ for the $BeCl_2$ solution. The slope
and curvature of the $\frac{1}{T_{2a}}$ line in Fig. 2 has been made identical to
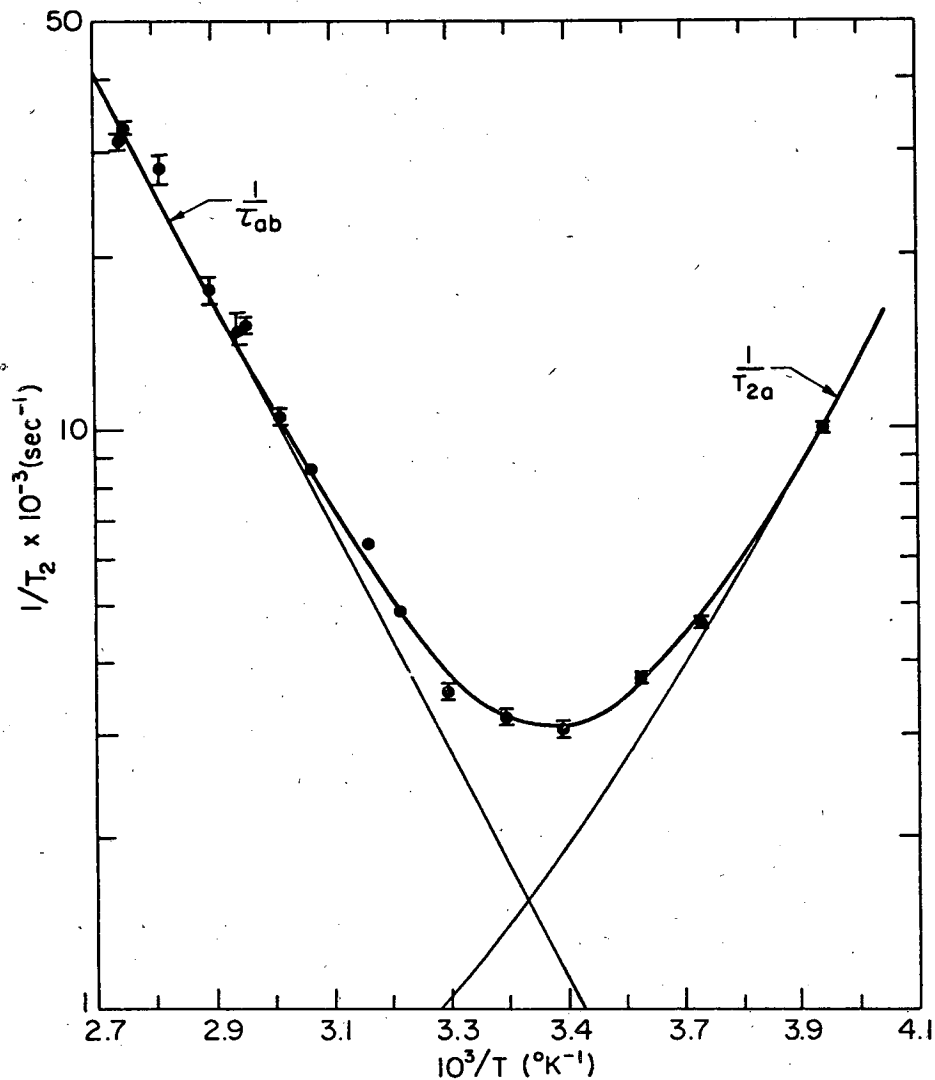
XBL714-6661

Fig. 2. Transverse relaxation rate of oxygen-17 in water in the first coordination sphere of beryllium ion versus reciprocal absolute temperature. Composition of solution was 0.40 gm $BeCl_2$(anhydrous), 0.20 gm $Mn(ClO_4)_2 \cdot 2H_2O$ and 0.913 gm H_2O enriched to 20% (46.5% $H_2^{18}O$) oxygen-17.
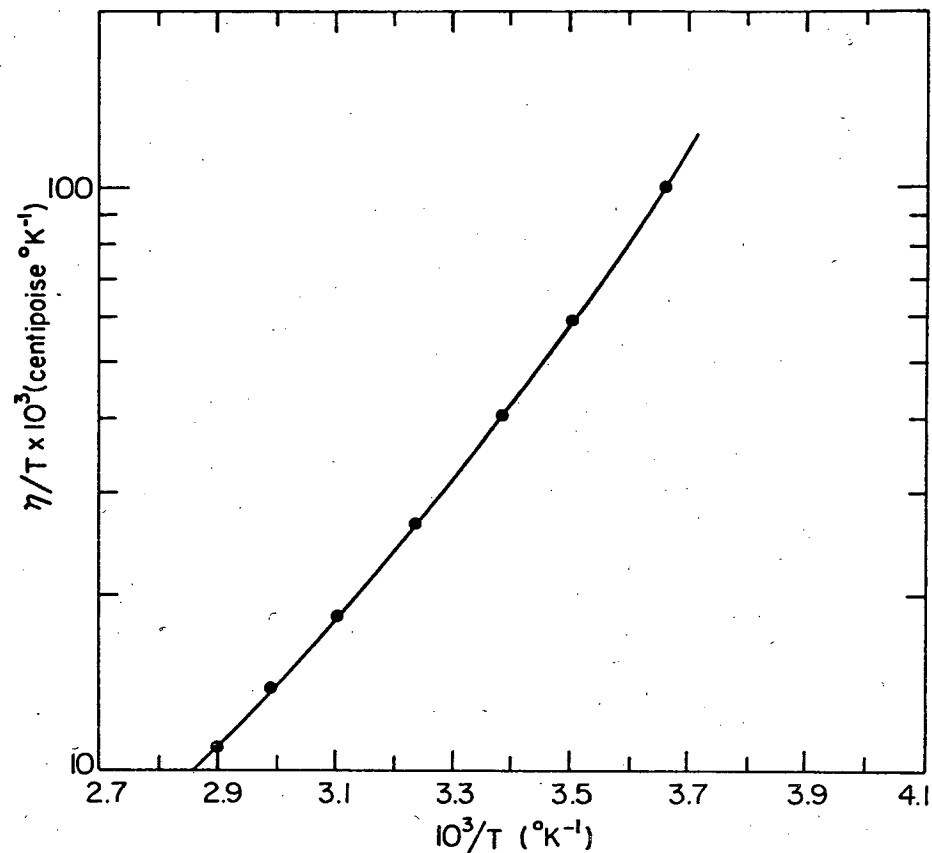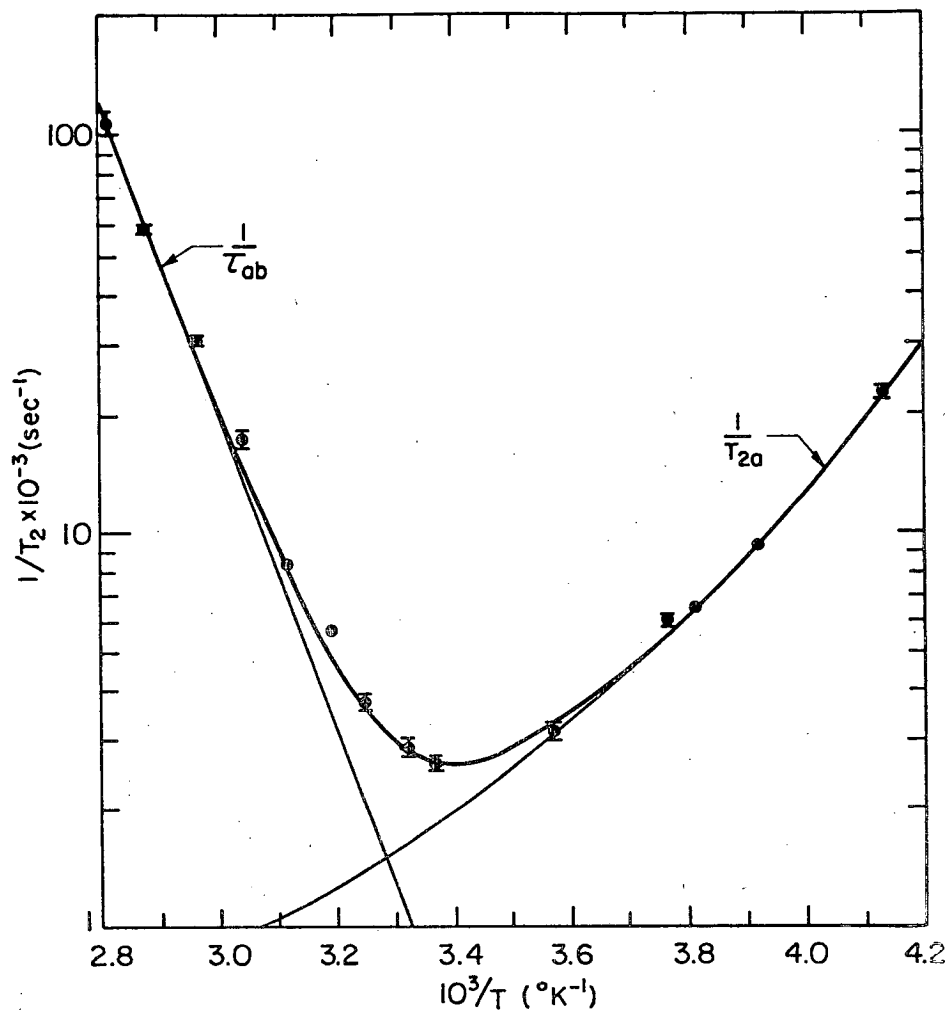

XBL714-6662

Fig. 3. Dependence of the ratio of viscosity and absolute temperature on the reciprocal of absolute temperature for a beryllium chloride solution of identical composition to that used in the nmr study.

that in Fig. 3. The T_{2a} region for Al^{3+} ion and $\frac{n}{T}$ measurements are

shown later to have identical slope and curvature over a rather long

temperature range, establishing the $\frac{n}{T}$ temperature dependence of this

region.

C. Gallium Ion

Figure 4 shows the linewidth as a function of temperature for the

waters in the first coordination sphere of gallium ion. The data show

the same behavior with temperature as do the data for beryllium ion.

The data can be seen to be the sum of two lines. The line labelled

$\frac{1}{\tau_{ab}}$ yields for $\Delta H^{\ddagger}$ and $\Delta S^{\ddagger}$ 16.5 Kcal/mole and +10 eu. respectively.

Extrapolation of the $\frac{1}{\tau_{ab}}$ line to $25°$ gives a first order reaction rate

constant for water exchange of 7.6×10^2 sec^{-1}. The slope and curvature

of the line labelled $\frac{1}{T_{2a}}$ have been made identical to those measured

experimentally for $\frac{n}{T}$ shown in Fig. 5. The agreement between the two

sets of data indicates the quadrupole interaction to be the mechanism

causing relaxation at low temperatures.

Values for the exchange rate and enthalpy and entropy of

activation have been reported previously[6b] which differ significantly

from those reported here. The attempt was made to shift the bulk water

signal relative to that of the bound by the addition of Co^{2+}. The

water exchange from Ga^{3+} was rapid enough that the bulk signal could

not be completely separated from that of the bound. The output was

least-squares fitted by computer in an attempt to measure the exchange

rate and its temperature dependence. This task becomes difficult

when $\frac{1}{T_{2a}}$ becomes comparable to or greater than $\frac{1}{\tau_{ab}}$. The previous

study only covered the temperature range from 10 to 56°C. From Fig.4

$\frac{1}{T_{2a}}$ and $\frac{1}{\tau_{ab}}$ are found to be nearly equal. It is not surprising

XBL714-6663

Fig. 4. Dependence of the transverse relaxation rate of oxygen-17 in the first coordination sphere of gallium ion on the reciprocal of absolute temperature. Sample composition was

1.06 gm $Ga(ClO_4)_3 \cdot 6H_2O$

0.32 gm $Mn(ClO_4)_2 \cdot 6H_2O$

1.00 gm 20.5% $H_2^{17}O$ (46.5% $H_2^{18}O$)
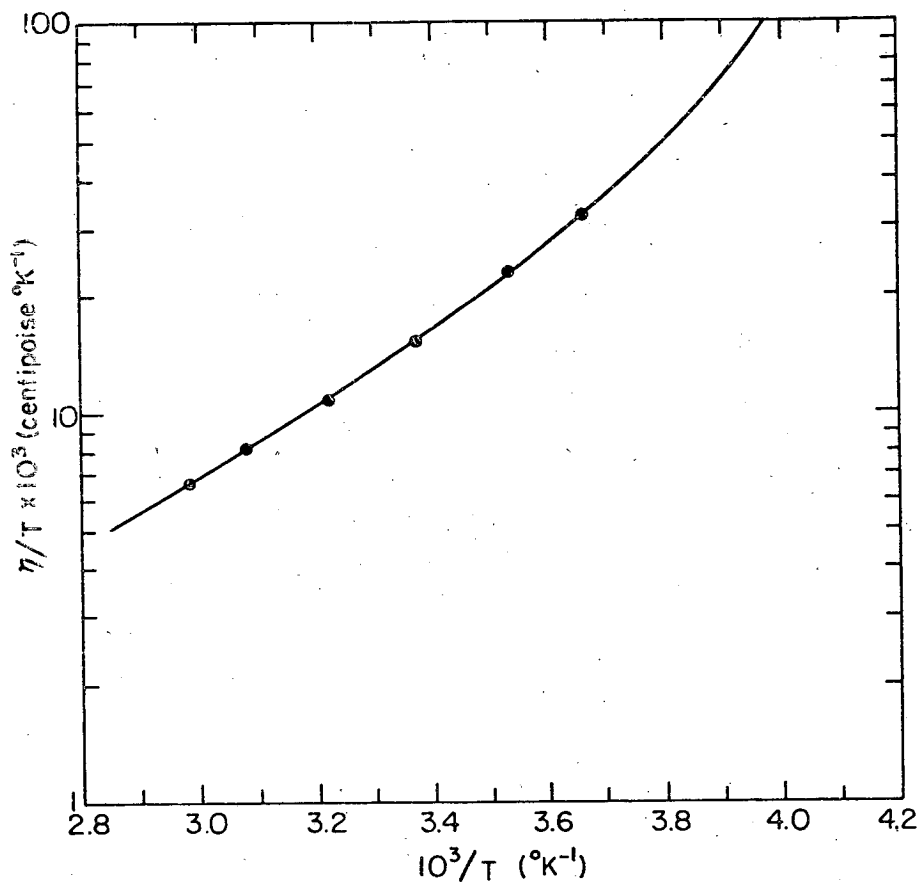
XBL714-6664

Fig. 5. $\frac{\eta}{T}$ versus $\frac{1}{T}$ for gallium perchlorate of identical composition to that used in nmr measurements.

therefore that serious errors were encountered in the previous study.

D. Aluminum Ion

The aluminum ion system has been thoroughly studied previously.[6a,b] The significant differences encountered with the Ga^{3+} system and the improved experimental conditions, encouraged a repetition of the previous work to extend the temperature range in order to determine a more exact $\Delta H^{\ddagger}$ and $\Delta S^{\ddagger}$. The results of a study of the bound water linewidths as a function of temperature from $0°$ to $140°C$ is shown in Fig. 6. The high temperature region where the linewidth is controlled by the rate of chemical exchange with the bulk solvent shows a temperature dependence which corresponds to an activation enthalpy of 15.6 Kcal/mole and an activation entropy of 0 eu. This result differs radically from the results reported previously.

Direct comparison of the earlier bound water linewidth data with those given here would indicate no unexplainable differences. The two sets of data differ by a constant factor at lower temperatures presumeably reflecting the viscosity differences of the two solutions. At higher temperatures where exchange determines the linewidth the data agree within the expected error limits. However the present data indicate a consistently faster exchange rate. If this is significant it could be due to the changes in sample composition.

The temperature dependence for water exchange given here would be expected to be much more accurate than that given previously because the present data cover a much larger temperature range and the exchange parameters are available in a very straightforward manner.

The value of the first order reaction rate constant at $25°C$ is found to be 16 sec^{-1} by extrapolation of the $\frac{1}{\tau_{ab}}$ line. This value
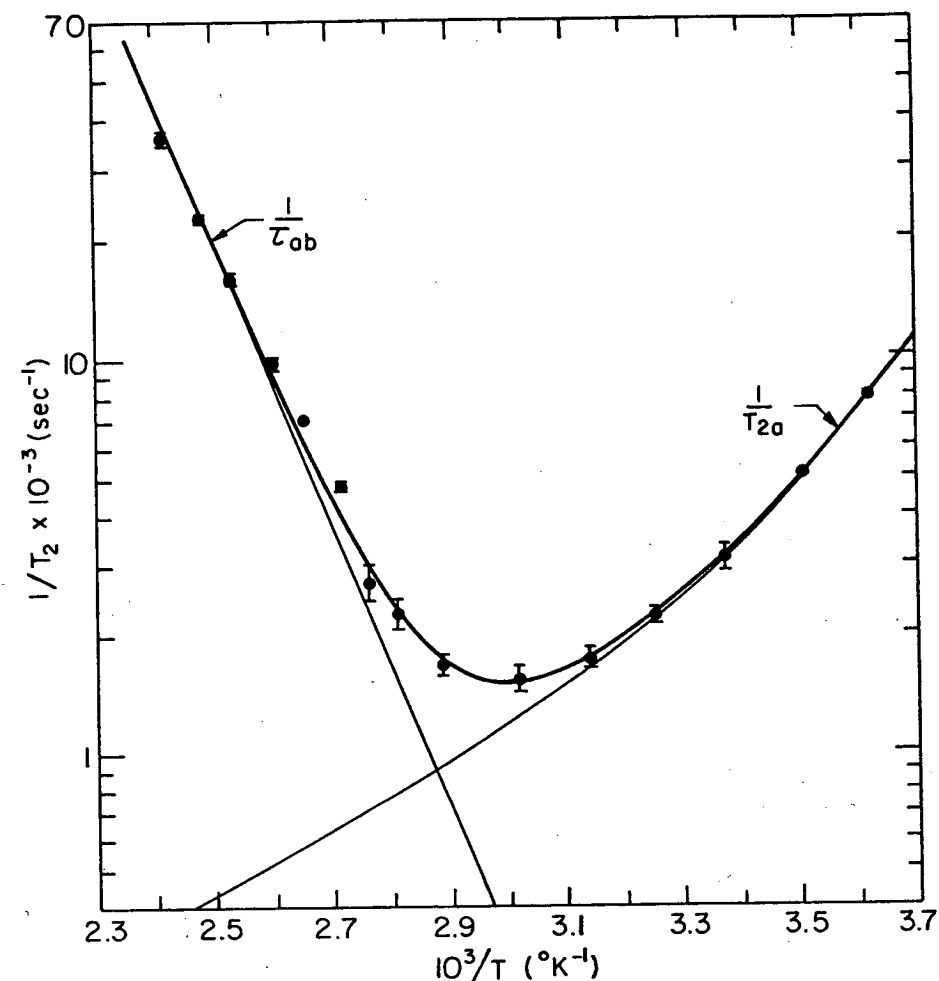
XBL714-6665

Fig. 6 Transverse relaxation rate of oxygen-17 in water in the first coordination sphere of Aluminum ion versus $\frac{1}{T}$. Composition of sample was

1.93 gm $Al(ClO_4)_3 \cdot 7H_2O$

0.30 gm $Mn(ClO_4)_2 \cdot 2H_2O$

1.31 gm 20.5% $H_2^{17}O$ (46.5% $H_2^{18}O$)

is open to considerably more uncertainty than the values for previous ions in this work due to the large temperature interval of the extrapolation. It is consistent with the earlier work of Hunt and Taube who found all waters had exchanged within three minutes[1b], and is also consistent with the results of Baldwin and Taube[23] who determined the rate constant to be less than 72 sec^{-1}.

For Al^{3+} ion it was possible to measure the $\frac{1}{T_{2a}}$ region over a large range of temperatures. The viscosity of the Al^{3+} solution has been measured over the same temperature range. A plot of $\frac{\eta}{T}$ versus $\frac{10^3}{T}$ is shown in Fig. 7. The temperature dependence of the two sets of data are seen to be essentially identical in the low temperature region when the $\frac{1}{\tau_{ab}}$ contribution is small. This would suggest some validity in the assumption that a macroscopic quantity such as viscosity is closely related to the resistance to tumbling experienced by a molecular sized species in aqueous solution. Other possible explanations for this effect will be discussed later. The correspondence of the temperature dependences also confirms that the quadrupole interaction of the ^{17}O with the electric field gradients surrounding it is responsible for the relaxation of oxygen-17 in the first hydration sphere of a diamagnetic metal ion.

E. Indium Ion

A typical oxygen-17 resonance signal for an In^{3+} solution is shown in Fig. 8. The intense broad signal is the resonance of oxygen-17 associated with indium ion. The nature of these oxygens will be discussed more fully later. The smaller narrower signal is the resonance of the naturally abundant oxygen-17 contained in the perchlorate anions. The perchlorate oxygen signal is shifted down field 272 ppm
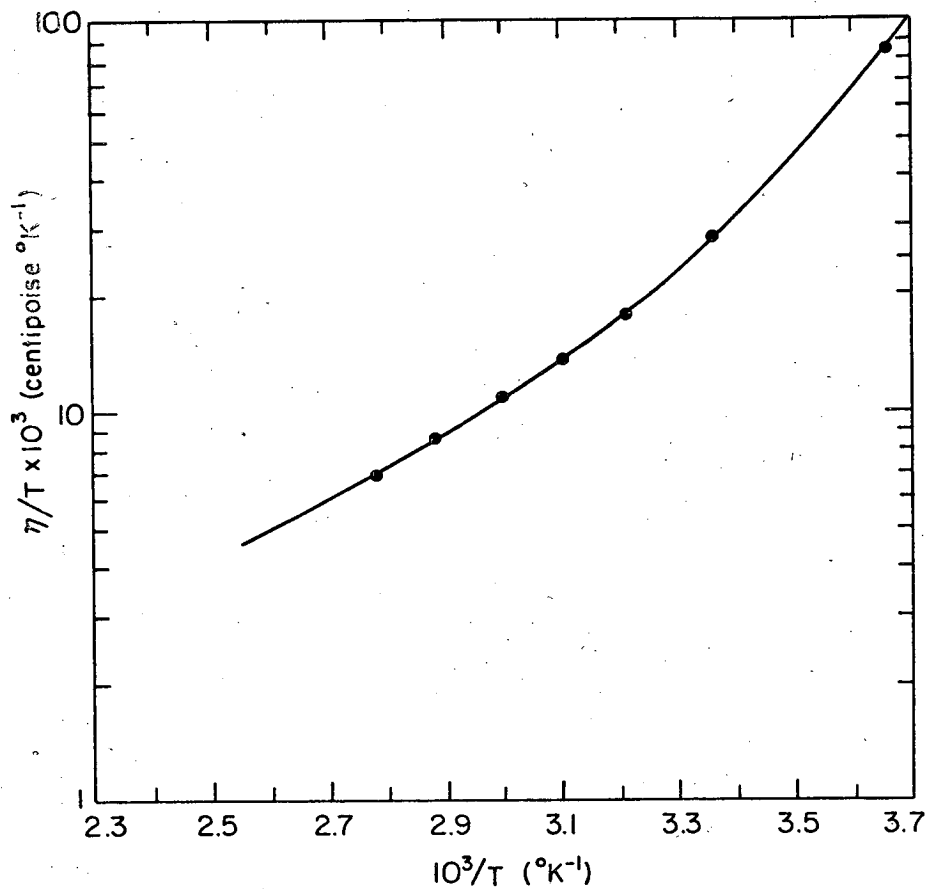
XBL 714 - 6666

Fig. 7. Viscosity over temperature versus reciprocal temperature for aluminum solution identical in composition to that given under Fig. 6.

XBL714-6667

Fig. 8. Oxygen-17 nmr resonance signal obtained from indium perchlorate solution defined under Fig. 9. The large broad signal is that of oxygen-17 associated with indium (III) in solution. The smaller narrower signal is that of the natural abundance oxygen-17 contained in the perchlorate anions in solution.

from the water oxygen-17 resonance (in pure water) in agreement with previous measurements.[24,25] The natural linewidth of the perchlorate signal is much narrower than that measured, because of modulational broadening. No attempt was made to measure this linewidth accurately. Little change was noted in the linewidth as a function of temperature from 0° to 100°C.

The overlapping signals make direct measurement of the transverse relaxation rate for the bound oxygen signal difficult. Accurate line-widths were obtained by a non-linear least-squares curve fit to the data assuming two overlapping derivative absorption lines. The line-widths calculated in this manner are shown in Fig. 9 as a function of temperature.

Again both regions predicted by Eq. 17 are observed. The line labelled $\frac{1}{\tau_{ab}}$ describes the rate constant for oxygen exchange from the In^{3+} ion. The exchange parameters are $\Delta H^{\ddagger} = 13$ Kcal/mole and $\Delta S^{\ddagger} = 6$ eu and the first order rate constant for oxygen exchange at 25°C is $k_{25°} = 1.7 \times 10^3$ sec^{-1}.

The number of oxygens per In^{3+} can be calculated by using the perchlorate oxygen-17 as an internal standard. Assuming these oxygens to be naturally abundant and knowing the percent enrichment of the water and the sample composition, the number of oxygens per indium ion can be calculated from the relative intensity of the two signals. This procedure for the salts dissolved in pure water yields about one oxygen for every sixteen indium ions. For this reason the perchlorate oxygen signal is much more prominent in this system compared to the previous cases where the perchlorate oxygen-17 signal was negligibly small.

Since so few indiums are contributing to the total bound oxygen signal, hydrolysis and/or complexation must somehow be involved.
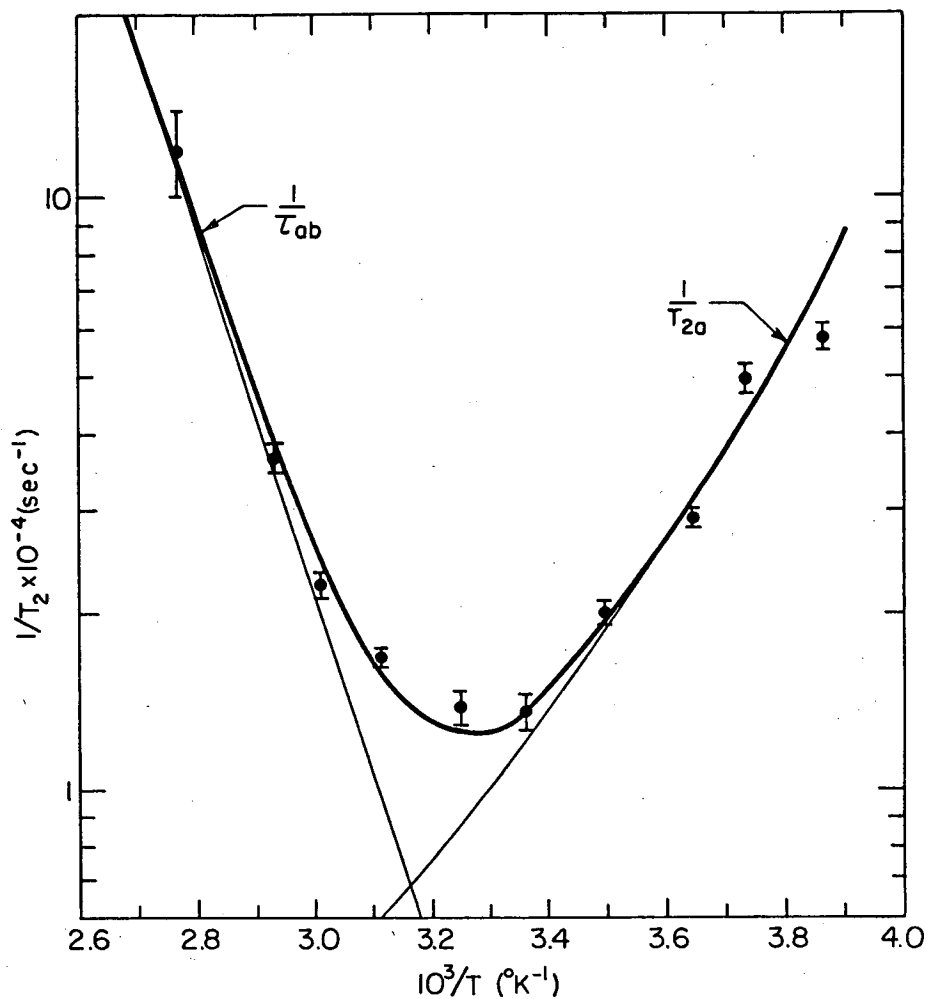
XBL 714-6668

Fig. 9. Dependence of the linewidth of the resonance signal of oxygen-17 associated with indium (III) in solution on reciprocal temperature. Sample composition was:

2.04 gm $In(ClO_4)_3 \cdot 5H_2O$

0.23 gm $Mn(ClO_4)_2 \cdot 2H_2O$

2.00 gm   20% $H_2^{17}O$ (48.7% $H_2^{18}O$)

Complexation of indium ions by perchlorate would be expected to increase the rate of water exchange due to the reduced effective charge felt by the remaining waters. However a large amount of complexation would be necessary with only one In^{3+} in every 100 or so free of complexing perchlorates. This possibility has been ruled out experimentally.[26] No complexation of In^{3+} by perchlorate could be observed by Raman spectroscopy while the In^{3+}-water interaction was observed.

Several percent of the total In^{3+} in this solution would be expected to be hydrolysed on the basis of measured hydrolysis constants.[27] Hydrolysis of an In^{3+} would be expected to increase the rate of water exchange of the waters coordinated to the hydrolysed species relative to those coordinated to an unhydrolysed In^{3+}. The waters coordinated to an unhydrolysed In^{3+} must be exchanging at least five times faster than the oxygens being observed because the intensity of the signal is insufficient to account for all the waters in the first hydration sphere of the unhydrolysed In^{3+}. A factor of five more rapid relaxation would make the signal from these oxygens unobservable under the present experimental conditions. A reasonable conclusion is that this signal is due to bound hydroxide ions attached to an In^{3+} ion. This is consistent with the expected degree of hydrolysis and the intensity of the oxygen-17 resonance signal. The addition of acid or base to the solution would be expected to have drastic effects on the intensity of the bound oxygen signal. This has been observed experimentally as shown in Table I.

Table I. Effect of acidity on oxygen-17 signal in indium (III) solutions

mmole H_2O	mmole In^{3+}	mmoles $HClO_4$	mmoles $NaHCO_3$	Intensity ClO_4^- / Intensity bound O^{17}
52.9	3	0	0	0.30
52.9	4	0	0	0.34
53.7	4	0.42	0	0.56
53.7	4	0.42	0.42	0.28
53.7	4	0.42	0.84	0.15

As acid is added the signal intensity ratio nearly doubles compared with the two cases containing only indium perchlorate and manganese perchlorate. The addition of sodium bicarbonate results in a progressively increasing bound water signal confirming the hypothesis that this signal is due to hydroxide ions bound to hydrolysed In^{3+} ions. The line labelled $\frac{1}{\tau_{ab}}$ in Fig. 9 measured as a function of temperature is the rate of exchange of the hydroxide ions from the hydrolysed indium ions. To increase the signal to noise the data in Fig. 9 were measured on a hydrolysed sample for which the integrated intensity indicated about one bound oxygen for every indium ion in solution. Fig. 8 is a signal from this solution.

Several mechanisms could be responsible for the rate of OH- exchange. The hydroxide ions could exchange directly with the bulk solvent. The reverse of the hydrolysis reactions or proton transfer within a hydrolysed species could occur. Either of these latter mechanisms would change a bound hydroxide into a bound water, which has already been shown to exchange rapidly, and cause the relaxation of the bound hydroxide.

Which of these possible mechanisms dominates in causing the exchange of hydroxide is not easily estimated. The rate of proton exchange from the first hydration sphere waters could in principle be measured by pmr. However this is only equal to the rate of the reverse hydrolysis reaction when the rate of water exchange is small compared to the proton exchange rate. In the case of indium the waters must be exchanging faster than the hydroxide, providing a path for proton exchange independent of the hydrolysis reactions. The activation enthalpy measured for the hydroxide exchange is not inconsistent with that measured for proton exchange from chromic ion[28] where

the rate of water exchange is small compared to that for protons. There appears to be no a priori reason for excluding any of these mechanisms from consideration at this time.

The exchange rate and $\Delta H^{\ddagger}$ extrapolated to room temperature may in fact be in appreciable error if more than one of these mechanisms is important over the temperature range covered. The exact data points could be more accurately fit by assuming two exchange lines with different slopes. However the accuracy of the data does not warrant such refinements. The $\Delta H^{\ddagger}$ given may be only an average of the $\Delta H^{\ddagger}$ for two mechanisms depending on the relative importance of each. In this case the k_{25° given would only be a lower limit to the actual first order reaction rate constant for hydroxide exchange.

The temperature dependence of the region of quadrupole relaxation has been taken from that measured experimentally for $\frac{\eta}{T}$ as shown in Fig. 10. The agreement with the temperature dependence of $\frac{1}{T_{2a}}$ confirms the quadrupole coupling mechanism as causing the relaxation.

Calculation of the expected quadrupole relaxation becomes even more difficult than in previous cases. The size of the hydrolysed species is open to considerable question. Not only are hydrolysed species containing one In^{3+} present but polymerized species containing several indium ions and several hydroxy bridges are present. The possibility exists that only the monomeric species would be observed by the present experiments due to the significantly slower tumbling time of the polymerized species. Smaller electric field gradients about the oxygen-17 nuclei in the hydroxy bridges could counteract the influence of longer tumbling times. The change of field gradients about oxygen-17 in these hydrolysed species is impossible to estimate. It is not possible to know if all the hydrolysed species are being
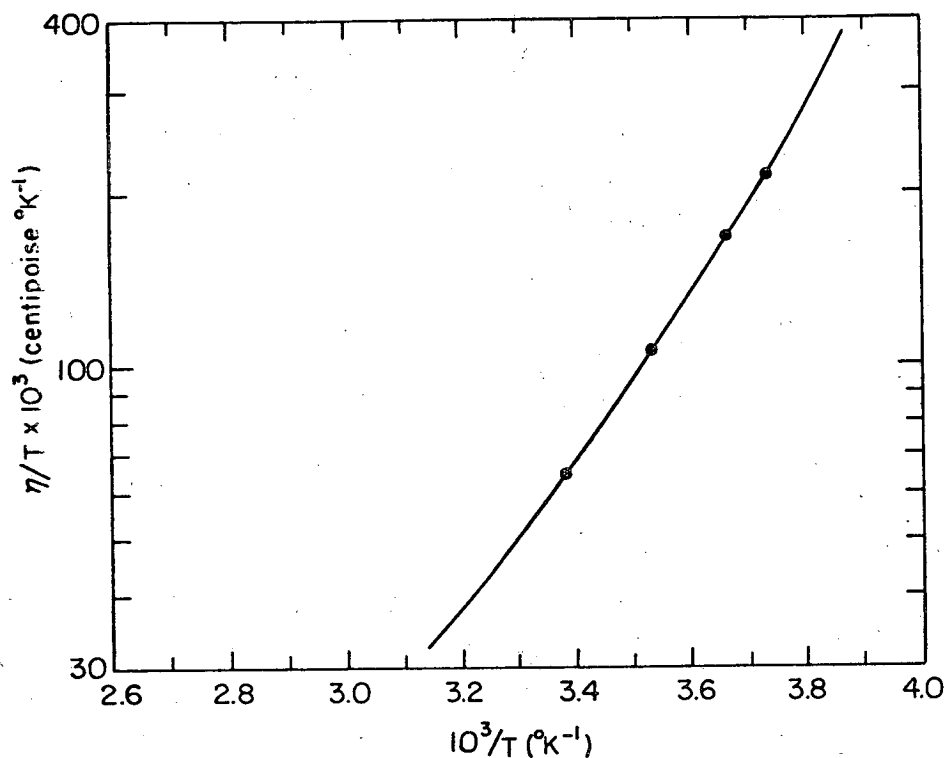
XBL 7/4-6669

Fig. 10. $\frac{\eta}{T}$ versus $\frac{1}{T}$ for indium perchlorate solution identical in composition to that used in nmr measurements.

observed. The equilibrium constants were determined in a medium of 3M $NaClO_4$. Different experimental conditions make exact calculations using hydrolysis constants of doubtful value for the relatively sensitive task of computing the exact amount of monomer relative to polymer species.

One piece of information which would tend to suggest only the monomeric species are being observed is available. Calculations assuming the same field gradients about a bound hydroxide as a bound water and assuming the radius of the hydrated complex is that appropriate to a hydrated In^{3+} indicate the same relative deviation from the experimental relaxation as observed in this work for other plus three ions. These calculated values are $\frac{1}{T_{2a}}$ (calc) = 1.6×10^5 sec^{-1} and $\frac{1}{T_{2a}}$ rot calc = 2.0×10^3 sec^{-1}. This would tend to suggest that only monomeric species were being observed and that the electric field gradients are mainly due to the close proximity of a highly charged ion. As discussed in discussion section A, this is one possible explanation of the magnitude of quadrupole relaxation measured for all the ions in this work.

Glass, Schwabacher and Tobias[29] attempted to measure the rate of water exchange from In^{3+} ion in acid solution where hydrolysis is nearly completely suppressed. The chemical shift of the bulk water was changed by the addition of Dy^{3+}. No bound water resonance could be resolved due to the rapid exchange of waters out of the first coordination sphere. However the rate of chemical exchange was estimated by the amount of broadening of the bulk water resonance caused by exchange with the magnetically different environment of the bound waters. Ignoring any relaxation occuring in the bound environment they calculated an average lifetime in the bound environment.

As discussed later in discussion section A estimates of the

amount of quadrupole relaxation occuring within the first hydration

sphere about a metal can be made. These figures for the present indium

solution have already been presented. Assuming the same deviation

from these calculated values as observed experimentally for other plus-3

ions, the entire linebroadening observed by Glass, et.al. can easily

be accounted for by quadrupole relaxation within the first hydration

sphere. Therefore no indication of the rate of water exchange can be

extracted from their data.

F. Thorium Ion

The bound oxygen-17 signals from solutions containing thorium ion

appear qualitatively similar to those obtained for indium as discussed

in the preceeding section. The oxygen-17 from natural abundance

contained in the perchlorate anions contributes a significantly intense

signal so that a non-linear least squares computer fit was necessary

to obtain the linewidth of the bound oxygen signal from the combined

lineshape.

The linewidth data are presented as a function of temperature in

Fig. 11. The temperature dependence of the $\frac{1}{T_{2a}}$ region has been

made identical to that measured for $\frac{n}{T}$ as shown in Fig. 12. The

exchange parameters for the bound oxygens are $\Delta H^{\ddagger} = 23 \pm 5$ kcal/mole,

$\Delta S^{\ddagger} = 40 \pm 15$ eu and $k_{25^\circ} = 7 \times 10^4$ sec^{-1}. These results are open to

considerably more uncertaintly than previous results in this report due

to the significantly smaller bound oxygen signal obtained from this
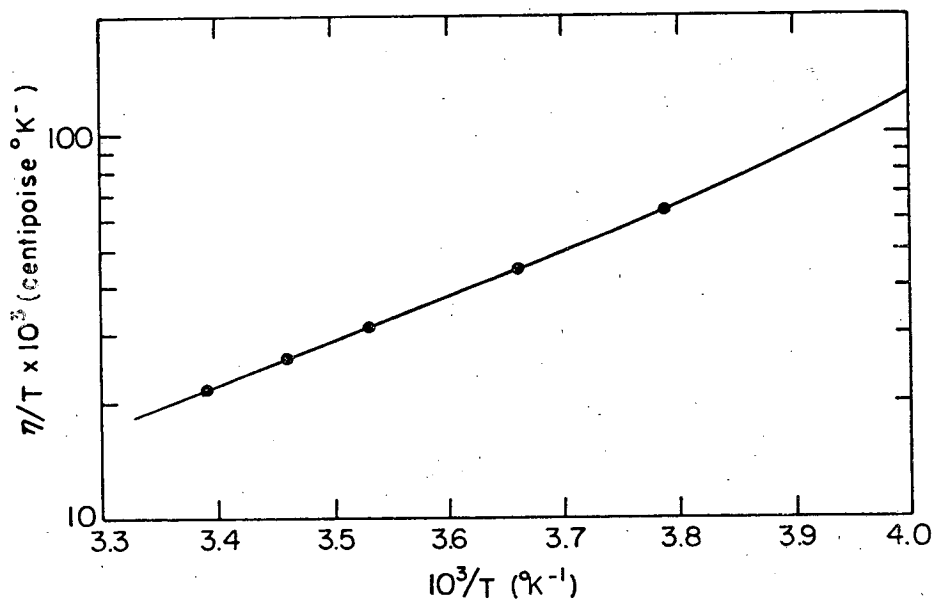
sample.

The number of observable oxygens bound to each thorium ion on the
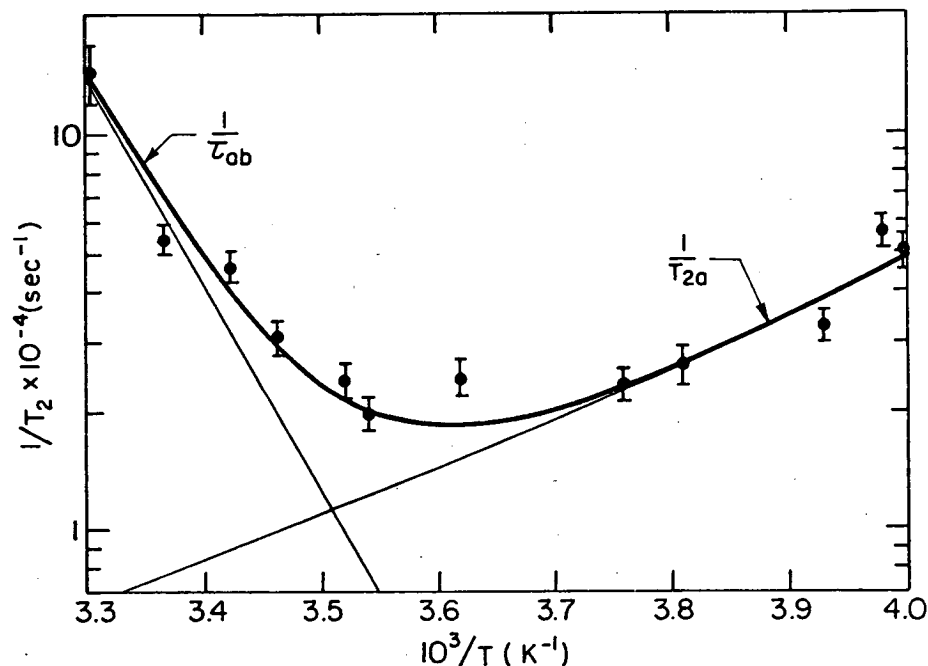
XBL714-6671

Fig. 11. $\frac{1}{T_2}$ versus $\frac{1}{T}$ for a thorium perchlorate solution of

composition:

1.00 gm Th(ClO$_4$)$_4$ (anhydrous)

0.40 gm Mn(ClO$_4$)$_2$· 2H$_2$O

1.00 gm 20% H$_2^{17}$O (46.5% H$_2^{18}$O)

XBL714-6672

Fig. 12. Viscosity over temperature versus reciprocal temperature for thorium perchlorate solution of composition given under Fig. 11.

average can be calculated from the relative intensities of the bound oxygen signal and the natural abundance oxygen-17 signal from the perchlorate ions. The bound oxygen-17 signal averaged 5 times more intense than the perchlorate signal which corresponds to one oxygen for every 22 thorium ions in solution.

The hydrolysis of thorium ion in solution has been carefully studied by Hietanen and Sillén for thorium chloride solutions in concentrations comparable to those in the present study.[30] Calculations using these hydrolysis constants would suggest that the bound oxygen-17 signal could well be due to the oxygen-17 contained in a hydrolysed thorium species.

The signal cannot be due to waters coordinated to the hydrolysed species. The waters coordinated to unhydrolysed Th^{4+} ions must be exchanging at least a factor of five faster than the observed oxygens to make them experimentally unobservable. The measured signal intensity is several orders of magnitude too low to account for the expected signal from these waters. The waters about a hydrolysed species would be expected to exchange even faster than those about an unhydrolysed species due to the reduced effective charge. Since bound waters on the Th^{4+} are unobservable, those bound to the hydrolysed thorium species should be unobservable as well.

Extensive complexation by perchlorate anions cannot explain the low intensity of the observed signal. Raman spectra of the perchlorate anion in concentrated solutions of thorium perchlorate have failed to show evidence of any complex formation.[31]

The nature of these hydrolysed species is not obtainable from the present nmr technique. Hietanen and Sillén have identified the major hydrolysis products as having the formulas Th_2OH^{7+} and $Th_2(OH)_2^{6+}$.

This would suggest that the bound hydroxides occur only as bridging groups in the formation of thorium dimers. The exchange rates measured would then apply to the exchange of these hydroxy bridge oxygens with the oxygens contained in the solvent. Since there are two hydroxy bridged species, the measured exchange rates and temperature dependences may well be weighted averages for the possible different kinds of hydroxy bridged species.

G. Ions for Which No Bound Water Resonance Could Be Observed

No bound water resonance signal could be observed for Zinc, Uranyl, Scandium(III) and Thallium(III) ions in aqueous solution. All samples were observed at several temperatures from room temperature to at least minus twenty degrees centigrade. The bulk water resonance could be observed in each case with a linewidth of at least 2×10^6 Hz. The lack of a bound water signal under the present experimental conditions implies that the exchange rate for these ions at -20°C must be greater than about $6 \times 10^5 \text{sec}^{-1}$.

DISCUSSION:

A. Quadrupole Relaxation of First Coordination Sphere Waters

The relaxation of oxygen-17 nuclei in pure water is due to quadrupole interaction interupted by molecular tumbling.[22a,b] Equations (18) and (19) predict an $\frac{\eta}{T}$ temperature dependence for this type of relaxation. The quadrupole coupling should be much more efficient for bound waters due to the slower tumbling time of waters in the first coordination sphere of diamagnetic metal ions. Linewidths in the low temperature region for several of the ions studied where the quadrupole relaxation should dominate have shown the same temperature dependence as values for $\frac{\eta}{T}$ measured on the same solution, which confirms the quadrupole mechanism.

The expected amount of quadrupole relaxation could be claculated using Eqs. (18) and (19) if the quadrupole coupling tensor in water molecules bound to a metal ion were known. The quadrupole coupling tensor in gaseous $HD^{17}O$ has been measured in the principle axis system to be[32]: $\chi_{xx} = 10.175$ MHz, $\chi_{yy} = -8.891$ MHz and $\chi_{zz} = -1.283$ MHz. The principle axis system is defined such that the Z axis lies in the plane of the water molecule and bisects the HOD angle and the Y axis intersects the oxygen nucleus and also lies in the plane of the molecule. The quadrupole tensor for gaseous $H_2^{17}O$ will be assumed to be identical to these values, which should be a very good approximation.

The effect of the close proximity of a charged ion on the tensor is extremely difficult to calculate. The contribution to the second derivative of the electric potential at the oxygen nucleus due to the charged ion can be calculated. However if there is an apprecible Sternheimer antishielding correction,[33] the calculated values could be

even of opposite sign and perhaps larger than the direct contribution.
Unfortunately there is no simple way to estimate this correction.

There is evidence that the quadrupole tensor in water changes
significantly depending upon the physical state of the water.[34] This
can be attributed to the differences in the amount of hydrogen bonding
in each state. A first coordination sphere water would be expected
to have fewer hydrogen bonds than a bulk water and the quadrupole
tensor could on this basis resemble that of a gaseous water more
closely than that of any other state.

Experimental evidence is also available indicating the presence
of a large electric field can induce changes in the quadrupole coupling
tensor.[35] Estimates of the magnitude of these perturbations are
difficult to make and no experimental measurements have been attempted
for the present case. This point will be disscussed more fully later.

For the present the assumption will be made that the quadrupole
coupling tensor of a gaseous water molecule is the same as that of
waters in the first coordination sphere of a hydrated metal ion. This
assumption is not made in the expectation that it is true but primarily
to provide a reference point for the following discussion.

The radius of the hydrated complex will be taken as the ionic
radius of the metal ion plus the ionic radius of oxygen plus the Van
der Waals radius of oxygen. These values are listed in Table I. The
viscosity was measured for each solution at 0°C. and the results can
be found in Appendix II.

Connick and Wuthrich[4] have presented evidence that water molecules
in the first coordination sphere of metal ions rotate rapidly enough
about the metal-oxygen axis to average appreciably the quadrupole tensor in

the X-Y plane of the water molecules. Assuming this to be the case, a
new quadrupole tensor will result with components of $\chi_{xx} = \chi_{yy} =$
0.642 MHz and $\chi_{zz} = -1.283$ MHz. These new components give a calculated
transverse relaxation rate a factor of 74 smaller than that assuming
no such rotation. The exact value of this reduction in relaxation has
even less reliability than the quadrupole tensor itself. The only
significant observation is that a reduction in relaxation is expected
with rapid rotation and the size of the effect is probably large enough
to be easily measured.

Calculations of the magnitude of the $\frac{1}{T_{2a}}$ relaxation for waters
in the first coordination sphere of metal ions using Eqs. (18) and (19)
(assuming no internal rotation of the coordinated waters) consistently
predict much more relaxation than is measured experimentally. If the
rotation of the water molecules about the metal-oxygen axis is assumed
to be rapid enough to average completely the quadrupole tensor in the
X-Y plane, the calculated values, based on the tensor of the gaseous
molecule, become consistently smaller than the observed relaxation.

The results of the calculations are summarized in Table I.

Table I. Calculated and Experimental Values for the Quadrupole Relaxation Occuring within the First Hydration Sphere

Metal Ion	Radius of Hydrated Complexes(Å) [+]	Calculated $1/T_{2a}$ (Sec^{-1})		Experimental $1/T_{2a}$ (sec^{-1})	$\dfrac{1/T_{2a}(exp)}{1/T_{2a} \text{ calc. with rotation}}$
		without rotation	with rotation*		
Ga^{3+}	3.42	2.1×10^4	2.8×10^2	3.9×10^3	14
Be^{2+}	3.15	5.8×10^4	7.8×10^2	3.4×10^3	4.4
Al^{3+}	3.31	5.6×10^4	7.4×10^2	9.0×10^3	12
Mg^{2+}	3.46	3.9×10^4	5.4×10^2	$< 2 \times 10^3$	< 3.7

*In these calculations the assumption has been made that the water molecules rotate rapidly enough about the metal-oxygen axis to average the components of the quadrupole tensor perpendicular to this axis. The calculations are carried out using a new tensor obtained from that for gaseous HD^{16}O by averaging the X and Y components.

[+] The values for the ionic radii for the metal ions are found in ref. 36.

Calculated and experimental values are all given for 0°C, except for for magnesium for which the data refer to -22°C. Only an upper limit can be given for the experimental $\frac{1}{T_{2a}}$ for Mg^{2+} since only the $\frac{1}{\tau_{ab}}$ region could be observed for the temperature range covered. The estimate of the upper limit for the experimental $\frac{1}{T_{2a}}$ was set equal to the estimated error in the linewidth at the lowest temperature. The viscosity of the Mg^{2+} solution was measured at 0°C. and calculated at -22° by assuming the same temperature dependence of the $\frac{1}{T_{2a}}$ region as that measured for Be^{2+}.

The assumptions made in the calculations of $\frac{1}{T_{2a}}$ are:

1. The tumbling of the hydrated complex is isotropic with respect to the principal axes of water.

2. The Stokes-Einstein equation (Eq. 19) accurately relates the macroscopic viscosity to the tumbling time of the hydrated complex.

3. The effective radius is equal to the radius of the metal ion plus the ionic radius of oxygen plus the Van der Waals radius of oxygen.

4. The quadrupole tensor of a water in the first coordination sphere of a metal ion is the same as in a gaseous water molecule.

5. Conditions of extreme narrowing exist so that Eq. 18 accurately describes the quadrupole relaxation.

X-ray evidence from hydrated solids would suggest that waters adjacent to a metal are in the most symmetrical possible arrangement about the metal ion. This would be expected to be true for hydrated ions in solution as well. The hydrated complex possesses a high degree of symmetry and no particular tumbling axis should be different from any other. The first assumption of isotropic rotation of the hydrated complex should be a very good approximation. This assumption should be much more accurate for the tumbling of hydrated complexes than for water itself.

No independent method of measuring the tumbling time of the hydrated complexes is available. Equation 19 is the only method available for calculating the tumbling time. The applicability of Eq. 19 is verified by the experimental coincidence of the temperature dependence of $\frac{1}{T_{2a}}$ at low temperatures and $\frac{\eta}{T}$. While the absolute value of the tumbling time may be in error, it is expected that the relative changes in tumbling time from one ion to the next should be more accurately predicted. As we shall see, any trends from one ion to the next not predicted by this theory probably cannot be attributed to inadequacies in Eq. 19.

The assumed effective radius is only a lower limit to the true effective radius. A probable complication would be the presence of a second sphere of oriented waters about the metal ions for a period of time of the order of the tumbling time or larger. This would tend to increase the effective radius of the tumbling complex and make the actual tumbling time slower than is calculated. Measurements in this laboratory strongly indicate that the exchange time out of the second cordination sphere about Cr^{3+} is the same order of magnitude as the tumbling time of the hydrated complex.[37] This effect could indeed be a major complication in the calculations and will be discussed more fully later.

The condition of extreme narrowing is indeed a valid assumption as can easily be shown. The condition of extreme narrowing requires $(\omega_o \tau_r)^2 \ll 1$. The square of the product of the precessional frequency of the nucleus and the rotational tumbling time must be much smaller than one. The tumbling time for these ions is of the order of magnitude of 10^{-9} to 10^{-10} sec. and the precessional frequency was $5.1 \times 10^7 \text{sec}^{-1}$.

Thus

$$(\omega_o \tau_r)^2 \cong (5 \times 10^{-2})^2 \text{ to } (5 \times 10^{-3})^2 \ll 1$$

and the extreme narrowing condition is verified.

As shown in Table I, without exception the experimental quadrupole relaxation is significantly smaller than that calculated from theory. Inadequacies in the Stokes-Einstein equation are unlikely to produce such large discrepancies - almost two orders of magnitude for Mg^{2+}. Much closer agreement between the Stokes-Einstein equation and experiment has been found for cases where the tumbling time has been measured.

Changes in the quadrupole coupling tensor from that of a gaseous water molecule are to be expected. Estimates of the magnitude and direction of the contribution to the second derivative of the electric potential at the oxygen nucleus from the presence of the charged ion would add a small negative term to χ_{zz} and a positive term half as large to χ_{xx} and χ_{yy}. This would have the effect of increasing the quadrupole relaxation (e.g. about one percent in the case of Mg^{2+}) rather than decreasing it as observed experimentally. Sternheimer antishielding corrections would be of opposite sign and probably even larger in magnitude than the direct ion effect, but there is no simple way to estimate the correction. The quadrupole relaxation has been observed to be much smaller than the calculated values for every case studied. Fortutious reduction of the relaxation by these electrostatic effects for every ion studied seems so unlikely that this possible explanation will not be considered.

Electric field induced perturbations of quadrupole interactions have been measured experimentally by Dixon and Bloombergen[35a,b].

The magnitude of these perturbations is difficult to estimate. Since significantly different electric fields are experienced by waters in the first coordination sphere of each of the ions studied, a large reduction of the observed relaxation in every case is difficult to explain by this mechanism

The most straightforward explanation which agrees most closely with experiment is the assumption of rotation of the water molecules causing at least partial averaging of the quadrupole tensor.

Examination of Table I shows a remarkable trend. The experimental $\frac{1}{T_{2a}}$ for the ions with the smallest charge are much closer to the calculated $\frac{1}{T_{2a}}$, assuming rotation. This is shown more exactly in the last column where the ratio of the experimental $\frac{1}{T_{2a}}$ to the calculated $\frac{1}{T_{2a}}$ with the rotation is given.

This trend can be explained by several mechanisms. The most straightforward explanation is that the data reflect the change in the electric field gradients about the oxygen-17 in the water molecule due to the close proximity of a charged ion. The electric field gradient due to the presence of the charged ion can be calculated and would tend to increase the amount of quadrupole relaxation. The larger the charge on the metal ion, the larger the gradient calculated, as observed experimentally. As mentioned previously the Sternheimer antishielding factor describing the distortion of inner shell electrons from spherical symmetry can have effects many times larger than the size of the direct interaction with the charge. Estimates of these effects are extremely difficult to make.

Dixon and Bloombergen[35a,b] have shown experimentally that the presence of an electric field can cause significant perturbations of

the quadrupole interaction in crystalline compounds. The fields available experimentally were many orders of magnitude smaller than those experienced by waters in the first hydration sphere of metal ions. The oxygen-17 quadrupole interaction has never been studied as a function of external electric field strength. But effects similar to those measured for the halogens would be expected. The magnitude is difficult to estimate due to the difference in electronic structure for oxygen and the very large electric fields in the present case. This effect also would be expected to show a distinct trend with charge. The trend in column 5 of Table I could well be explained in terms of changes in the electric field gradients about the oxygen-17 nucleus.

Other factors could possibly be causing the observed trend. Consider the effect of the charged ion on the waters immediately outside the first coordination sphere. These waters are far enough away that the variation in the radius of the ions no longer has much influence on their behavior. The main influence is the size of the charge. Shown in Table II is the quantity $\frac{z}{(r + 4.2)^2}$, where z is the charge on the metal ion, r is the ionic radius of the metal ion and 4.2 is the sum of the ionic radius of oxygen and two Van Der Waals radii of oxygen. This quantity is proportional to the force felt by waters outside the first coordination sphere at the distance indicated due to the presence of the charged ion.

Table II. Ionic Influence in Second Coordiantion Sphere

Metal Ion	$r(\text{Å})$	$\frac{z}{(r + 4.2)^2}$ (esu Å^{-2})	$\dfrac{1/T_{2a} \text{ exp}}{1/T_{2a} \text{ calculated with rotation}}$
Be^{2+}	0.35	0.10	4.4
Ga^{3+}	0.62	0.13	14
Mg^{2+}	0.66	0.08	< 3.7
Al^{3+}	0.51	0.13	12

The order of increasing $\frac{z}{(r + 4.2)^2}$ is seen to parallel closely that for increasing discrepancy between experimental and calculated $\frac{1}{T_{2a}}$. This suggests that the effect being observed is the presence of coordination spheres which maintain their integrity for periods of time comparable to the tumbling time of the complex. The effect increases the effective radius of the tumbling complex and slows the rate of tumbling. A longer tumbling time would cause greater relaxation than would be predicted by a model ignoring the presence of a second coordination sphere.

The presence of these more tightly held second coordination spheres could have the additional effect of hindering the free rotation of the first sphere waters. The incomplete averaging of the quadrupole tensor assumed earlier would produce a great deal more relaxation than would be expected assuming complete averaging. This effect would have the same trend with charge as that shown in Table II. The presence of a second coordination sphere could be expected to have a double effect on the amount of quadrupole relaxation of a first hydration sphere water.

Either change in the electric field gradients or the presence of a second hydration sphere is capable of explaining the observed results. Nothing definite can be said without knowledge of the exact quadrupole coupling tensor for coordinated water molecules.

B. Electrostatic Water Exchange Theory

Measurements and estimates of the rates of water exchange from many different metal ions can be found in the literature. Obviously no simple theory is capable of correlating all of the various cases since many different effects are capable of influencing the exchange

rate. Forces such as crystal field stabilization of ligands for transition series metals and covalent bonding can have measurable (and sometimes drastic) effects on the exchange rate. In most cases the electrostatic attraction of the charged metal ion for the electric dipole of the water molecule appears to be the dominant influence in determining the rate of water exchange.[3] Therefore an electrostatic model should prove valuable in the correlation of exchange data.

Assuming the only interaction between a water molecule and an ion is the electrostatic attraction between a charge and a dipole and that the activation process consists merely of separating partially a water from the metal ion, the free energy of activation can be shown to be

$$\Delta F^{\ddagger} = -\frac{Ze\mu}{D}\left(\frac{1}{r_2^2} - \frac{1}{r_1^2}\right) = +\frac{Ze\mu(r_2-r_1)(r_1+r_2)}{D\, r_1^2 r_2^2} \tag{1}$$

where Z is the charge of the metal ion, e is the basic unit of electric charge, μ is the dipole moment of the water molecule, D is the effective dielectric constant, and r_1 and r_2 are the separation of the metal ion and the oxygen in the hydrated ion and in the activated complex, respectively.

Defining $\frac{r_1+r_2}{2} = d$ and $r_2-r_1 \equiv \Delta r$ and letting $r_1 r_2 \approx d^2$, Eq. 1 reduces to

$$\Delta F^{\ddagger} = +\frac{Ze\mu}{D}\frac{2\Delta r}{d^3} \quad . \tag{2}$$

The reaction rate constant for water exchange is given by:

$$k_r = \frac{kT}{h} e^{-\frac{\Delta F^{\ddagger}}{kt}} \tag{3}$$

where all the symbols have the usual meaning. Eq. 3 can be rewritten as

$$-\log k_r + \log \frac{kT}{h} = \frac{2Ze\mu\Delta r}{2.303kTd^3 D} \quad . \tag{4}$$

The quantity r_1 will be taken to be the sum of the ionic radius of the metal ion and the ionic radius of oxygen.

The exact value of Δr is of little consequence for the following discussion. For the purposes of numerical evaluation, the physically reasonable value of 0.5 Å is chosen. A more critical assumption is that Δr remains unchanged from one ion to the next. The upper limit on Δr would be on the order of an Ångstrom since larger distances would leave sufficient opening in the first coordination sphere for another water to enter with no steric interference. Similar geometrical arguments suggest that values for Δr much smaller than 0.5 Å leave insufficient space for the entry of a new water into the first hydration sphere. Changes in Δr larger than about a factor of two are not expected and Δr might quite reasonably (within these expected limits) be assumed to be constant from one ion to the next.

This electrostatic model predicts that a plot of $\log k_r$ vs. $\frac{Z}{d^3}$ should yield a straight line if the above assumptions hold. Such a plot for a number of metal ions is shown in Fig. 13. As was pointed out in the discussion of several of the cations in this work, water exchange rates inferred from measurements by sound absorption or temperature-jump techniques differ significantly from exact measurements made by nmr. For this reason only ions for which accurate nmr data are available have been included in Fig. 13. The references and exact values are given in Appendix II. The ions marked with closed
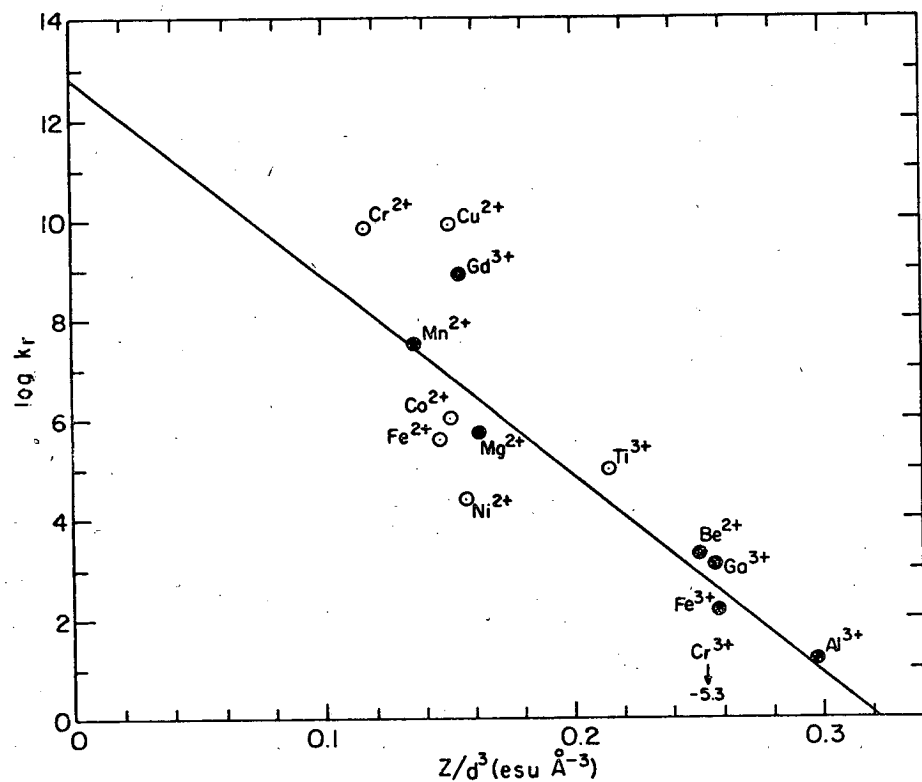
XBL714-6670

Fig. 13. Log k_r for water exchange versus $\frac{z}{d^3}$ for various metal ions in aqueous solution. Meaning of symbols is explained in the text.

circles are all the cases for which no ligand field stabilization is expected and should therefore provide the best examples for the electrostatic model. One additional point can be added to the plot since the log k_r intercept is given by the theory as log $\frac{kT}{h}$ = 12.8 at 25°C. With the exception of Gd^{3+} all the closed circles can be seen to fall very closely along a straight line as predicted by the theory.

The ions marked with open circles are all first row transition series. The ions falling below the line, Ni^{2+} and Cr^{3+}, can be explained by ligand field stabilization effects which increase the activation energy for either removing or adding a water molecule. Similar arguments for Co^{2+} and Fe^{2+} suggest a lowering of the activation energy leading to faster water exchange than predicted by electrostatics alone. This effect is not observed. These ions do not appear to differ significantly from a purely electrostatic exchange rate.

The unusually rapid exchange for chromous and cupric ions has been noted previously and explained in terms of the Jahn-Teller distortion of the octahedra of water molecules about the hydrated ions.[38] The same argument applies to Ti^{3+} except that the increase in exchange rate is not expected to be as great because the Jahn-Teller distortion of the first coordination sphere is much smaller. In agreement with these predictions titanous is observed to lie much closer to the line than either Cu^{2+} or Cr^{2+}.

With explainable exceptions all the known water exchange rates appear to be consistent with an electrostatic mechanism for determination of the rate of water exchange with the single exception of Gd^{3+}. The Gd^{3+} exchange rate suggests that either all the other examples thus far measured have been fortuitously chosen or that some unexpected effect makes the Gd^{3+} exchange rate in some way unusual.

The former seems most unlikely since the cations thus far measured

cover a very wide range of exchange rates and ionic radii.

The electrostatic model assumes the activation energy is due

to the difficulty of removing a water molecule from the vicinity of a

cation. Since this model appears to predict correctly many of the

rates thus far measured, an Sn1 mechanism for water exchange may appear

to be implied. No understanding of the detailed mechanism of water

exchange should be inferred from these results. An electrostatic model

based on the energy of the entering as well as the leaving water could

well predict results similar to those derived from the present model.

ACKNOWLEDGEMENTS

REFERENCES

1a. J. F. Hinton and E. S. Amis, Chem. Rev. $\underline{67}$, 367(1967)

b. J. P. Hunt and H. Taube, J. Chem. Phys. $\underline{19}$, 602(1951)

c. R. A. Plane and H. Taube, J. Phys. Chem. $\underline{56}$, 33(1952)

2a. W. Plumb and G. M. Harris, Inorganic Chem. $\underline{3}$, 542(1964)

b. R. K. Murmann and J. C. Sullivan, ibid. $\underline{51}$, 4506(1969)

3. T. J. Swift and R. E. Connick, J. Chem. Phys. $\underline{37}$, 307(1962); ibid. $\underline{44}$, 2553(1964)

4. R. E. Connick and K. Wüthrich, ibid. $\underline{51}$, 4506(1969)

5. Jackson, Lemons and Taube, ibid. $\underline{32}$, 553(1960)

6a. D. Fiat and R. E. Connick, ibid. $\underline{39}$, 1349(1963)

6b. D. Fiat and R. E. Connick, J. Amer, Chem. Soc. $\underline{90}$, 608(1968)

7. A. Fratiello, R. E. Lee, V. M. Nishida and R. E. Schuster, J. Chem. Phys. $\underline{48}$, 3705(1968); and references contained therein.

8. R. G. Wawro and T. J. Swift, J. Amer. Chem. Soc. $\underline{90}$, 2792(1968)

9. F. Bloch, Phys. Rev. $\underline{70}$, 460(1946)

10. J. V. Acrivos, J. Chem. Phys. $\underline{36}$, 1097(1962); and references therein

11. N. Bloembergen, Nuclear Magnetic Relaxation (M. Nijhoff. the Hague 1948) reprinted 1961

12. Abramowitz and Segun, eds., Handbook of Mathematical Functions, (Dover Publications, New York 1965) pp. 365

13. H. M. McConnell, J. Chem. Phys. $\underline{28}$, 430(1958)

14. A. Abragam, Principles of Nuclear Magnetism, (Oxford Press, 1961) pp 313-314

15. A. Abragam, Op. Cit., P. 298

16. N. A. Matwiyoff and H. Taube, J. Amer. Chem. Soc. $\underline{90}$, 2796(1968)

17. S. Nakamura and S. Meiboom, ibid. $\underline{89}$, 1765(1967)

18. M. Eigen and K. Tamm, Z. Electrochem. $\underline{66}$, 107(1962)

19. M. Eigen and G. G. Hammes, J. Amer. Chem. Soc. $\underline{82}$, 5951(1960)

20. H. Diebler, M. Eigen and G. G. Hammes, Z. Naturforsch $\underline{15b}$, 554(1960)

21. G. Atkinson and S. Petrucci, J. Phys. Chem. $\underline{70}$, 3122(1966)

22a. S. Meiboom, J. Chem. Phys. $\underline{34}$, 375(1961)

b. B. B. Garrett, A. B. Denison and S. W. Rabideau, J. Phys. Chem. $\underline{71}$, 2606(1967)

23. H. W. Baldwin and H. Taube, J. Chem. Phys. $\underline{33}$, 206(1960)

24. Mohammed Alei, Jr., J. Phys. Chem. __, 2904(1966)

25. B. N. Figgis, R. G. Kidd and R. S. Nyholm, Proc. Roy. Soc. (London) $\underline{A269}$, 469(1962)

26. R. E. Hester, R. A. Plane and G. E. Walrafen, J. Chem. Phys. $\underline{38}$, 249(1963)

27. G. Biedermann, Arkiv. för Kemi $\underline{9}$, 277(1956)

28. Ronald Tse Lee, Lawrence Radiation Laboratory Report, UCRL-19639

29. Gary E. Glass, William B. Schwabacher and R. Stewart Tobias, Inorganic Chem. $\underline{7}$, 2471(1968)

30. Sirkka Hietanen and Lars Gunnar Sillén, Acta Chemica Scandinavica $\underline{13}$, 533(1959)

31. R. E. Hester and R. A. Plane, Inorganic Chem. $\underline{3}$, 769(1964)

32. J. Verhoeven, A. Dymanus and H. Bluyssen, J. Chem. Phys. $\underline{50}$, 3330(1969)

33. R. M. Sternheimer, Phys. Rev. $\underline{84}$, 244(1951); $\underline{86}$, 316(1952); $\underline{95}$, 736(1954)

34. H. W. Spiess, B. B. Garrett, R. K. Sheline and S. W. Rabideau, J. Chem. Phys. $\underline{51}$, 1201(1969)

35a. R. W. Dixon and N. Bloembergen, J. Chem. Phys. 41, 1720(1964)

  b. R. W. Dixon and N. Bloembergen, ibid. 41, 1739(1964)

36. Handbook of Chemistry and Physics, 47th. Edition, R. C. Weast et.al.

    Eds..(Chemical Rubber Publishing Company, Cleveland, Ohio, 1966)

    pp. F124

37. W. L. Earl, IMRD Annual Report 1968, UCRL-18735 pp. 16

38. Charles Waymond Meredeth, Ph.D. Thesis, Lawrence Radiation

    Laboratory Report UCRL-11704

APPENDIX I

Proposition: $\displaystyle\sum_{n=0}^{\infty} n^2 J_n^{\ 2}(\beta) = \frac{\beta^2}{4}$

Proof:

$$J_n(\beta) = \frac{\left(\frac{\beta}{2}\right)^n}{n!} - \frac{\left(\frac{\beta}{2}\right)^{n+2}}{(n+1)!} + \frac{\left(\frac{\beta}{2}\right)^{n+4}}{2!\,(n+2)!} - \frac{\left(\frac{\beta}{2}\right)^{n+6}}{3!\,(n+3)!} + \frac{\left(\frac{\beta}{2}\right)^{n+8}}{4!\,(n+4)!} - \cdots$$

Squaring this series and collecting like powers of $\frac{\beta}{2}$ and multiplying by n^2 gives

$$n^2 J_n^{\ 2}(\beta) = \frac{\left(\frac{\beta}{2}\right)^{2n} n^2}{n!\,n!} - \frac{2\left(\frac{\beta}{2}\right)^{2n+2} n^2}{n!\,(n+1)!} + \left(\frac{\beta}{2}\right)^{2n+4} n^2 \left(\frac{1}{(n+1)!\,(n+1)!} + \frac{2}{2!\,n!\,(n+2)!}\right)$$

$$- 2\left(\frac{\beta}{2}\right)^{2n+6} n^2 \left(\frac{1}{2!\,(n+1)!\,(n+2)!} + \frac{1}{3!\,(n+3)!\,n!}\right)$$

$$+ \left(\frac{\beta}{2}\right)^{2n+8} n^2 \left(\frac{1}{2!\,2!\,(n+2)!\,(n+2)!} + \frac{2}{3!\,(n+3)!\,(n+1)!} + \frac{2}{4!\,(n+4)!\,n!}\right) + \cdots$$

$$= \sum_{\substack{j,k=0 \\ k \geq j}}^{\infty} \frac{(-1)^k \left(\frac{\beta}{2}\right)^{2(n+k)} n^2}{(n+j)!\,(n+k-j)!\,j!\,(k-j)!}$$

Summing over the values of n and collecting like powers of $\frac{\beta}{2}$ gives

$$\sum_{n=0}^{\infty} n^2 J_n^{\ 2}(\beta) = \left(\frac{\beta}{2}\right)^2 + \left(\frac{\beta}{2}\right)^4 \left(\frac{2^2}{2!\,2!} - \frac{2}{2!}\right)$$

$$+ \left(\frac{\beta}{2}\right)^6 \left[\frac{3^2}{3!\,3!} - \frac{2\cdot 2^2}{2!\,3!} + \frac{1}{2!\,2!} + \frac{2}{2!\,3!}\right]$$

$$+ \left(\frac{\beta}{2}\right)^8 \left(\frac{4^2}{4!\,4!} - \frac{2\cdot 3^2}{3!\,4!} + \frac{2^2}{3!\,3!} + \frac{2\cdot 2^2}{2!\,2!\,4!} - \frac{2}{2!\,2!\,3!} - \frac{2}{3!\,4!}\right) + \cdots$$

$$= \frac{\beta^2}{4}$$

Data for Magnesium Perchlorate Solution

Sample Composition: 1.00 gm $Mg(ClO_4)_2$

0.30 gm $Mn(ClO_4)_2 \cdot 6H_2O$

1.30 gm 20.5% $H_2^{17}O$ (46.5% $H_2^{18}O$)

Relaxation Data:

Temperature ($^{\circ}$C)	$10^3/T(^{\circ}K^{-1})$	$\frac{10^{-3}}{2\pi T_2}$ (Hz)	$\frac{10^{-4}}{T_2}$ (sec^{-1})
23.0	3.377	85 ± 8	46 ± 4*
14.1	3.482	40 ± 4	25 ± 2
0.7	3.672	18.5 ± 1	10 ± 0.7
-12.6	3.839	7.0 ± 0.5	3.8 ± 0.3
-22.0	3.980	3.3 ± 0.2	1.8 ± 0.1

Viscosity Data:

viscosity at 0°C is 4.0 centipoise

*The uncertainties represent one standard diviation for the computer

fit to the data.

APPENDIX II

II. Experimental Data

Data for Beryllium Chloride Solution

Sample Composition: 0.40 gm $BeCl_2$ (anhydrous)

0.20 gm $Mn(ClO_4)_2 \cdot 2H_2O$

0.913 gm 20% $H_2^{17}O$ (46.5% $H_2^{18}O$)

Relaxation Data:

Temperature (°C)	$10^3/T$ (°K^{-1})	$\frac{10^{-1}}{2\pi T_2}$ (Hz)	$\frac{10^{-3}}{T_2}$ (sec^{-1})
91.0	2.746	51 ± 2	32 ± 1
91.0	2.746	53 ± 2	33 ± 1
82.0	2.816	45 ± 3	28 ± 2
72.1	2.897	28 ± 2	18 ± 1
66.2	2.947	24 ± 2	15 ± 1
65.9	2.950	24.5 ± 0.7	15.4 ± 0.5
58.6	3.015	17.0 ± 0.7	10.7 ± 0.5
53.4	3.063	13.7 ± 0.3	8.6 ± 0.2
43.4	3.160	10.2 ± 0.1	6.4 ± 0.1
38.1	3.213	7.8 ± 0.1	4.9 ± 0.1
30.2	3.297	5.7 ± 0.3	3.6 ± 0.2
21.2	3.398	5.1 ± 0.3	3.2 ± 0.2
13.2	3.493	4.8 ± 0.2	3.0 ± 0.2
2.7	3.626	6.0 ± 0.3	3.8 ± 0.2
-5.1	3.731	7.4 ± 0.4	4.7 ± 0.2
-19.2	3.939	16.2 ± 0.3	10.2 ± 0.2

Viscosity Data:

Temperature (°C)	$10^3/T$ (°K^{-1})	$\eta/T \times 10^3$ (centipoise °K^{-1})
72.4	2.89	10.9
61.4	2.99	13.8
49.5	3.10	18.3
35.9	3.23	26.5
22.3	3.39	41.0
12.5	3.51	58.9
0.0	3.66	100

Data for Gallium Perchlorate Solution

Sample Composition: 1.062 gm $Ga(ClO_4)_3 \cdot 6H_2O$

0.325 gm $Mn(ClO_4)_2 \cdot 6H_2O$

1.00 gm 20.5% $H_2^{17}O$ (46.5% $H_2^{18}O$)

Relaxation Data:

Temperature (°C)	$10^3/T$ (°K^{-1})	$\frac{1}{2\pi T_2} \times 10^{-2}$ (Hz)	$\frac{1}{T_2} \times 10^{-3}$ (sec^{-1})
81.9	2.817	173 ± 10	109 ± 62
74.3	2.878	93 ± 3	59 ± 2
64.4	2.963	49 ± 1	31 ± 1
56.0	3.039	28 ± 1	17 ± 1
47.9	3.115	13.4 ± 0.3	8.4 ± 0.2
40.5	3.189	9.0 ± 0.1	5.68 ± 0.06
34.9	3.245	6.0 ± 0.3	3.8 ± 0.2
28.7	3.320	4.6 ± 0.2	2.9 ± 0.1
23.8	3.365	4.1 ± 0.2	2.6 ± 0.1
7.0	3.570	5.1 ± 0.3	3.2 ± 0.2
-7.4	3.764	9.6 ± 0.5	6.0 ± 0.3
-10.8	3.812	10.4 ± 0.2	6.5 ± 0.1
-18.0	3.920	14.9 ± 0.3	9.3 ± 0.2
-31.0	4.131	35.9 ± 1	22.6 ± 1

Viscosity Data:

Temperature (°C)	$10^3/T$ (°K^{-1})	$\eta/T \times 10^3$ (centipoise °K^{-1})
62.3	2.98	6.68
51.1	3.08	8.28
37.4	3.22	10.9
23.5	3.37	15.5
10.2	3.53	23.2
0.0	3.66	32.5

Data for Aluminum Perchlorate Solution

Sample Composition: 1.933 gm $Al(ClO_4)_3 \cdot 7H_2O$

0.297 gm $Mn(ClO_4)_2 \cdot 2H_2O$

1.310 gm 20.5% $H_2^{17}O$ (46.5% $H_2^{18}O$)

Relaxation Data:

Temperature (°C)	$10^3/T$ (°K^{-1})	$\frac{10^{-2}}{2\pi T_2}$ (Hz)	$\frac{10^{-3}}{T_2}$ (sec^{-1})
141.2	2.413	58 ± 2	36 ± 1
129.3	2.484	36 ± 1	23 ± 1
121.8	2.538	25.5 ± 0.7	16.0 ± 0.4
111.0	2.603	15.7 ± 0.6	9.8 ± 0.4
104.2	2.650	11.2 ± 0.3	7.0 ± 0.2
95.4	2.713	7.7 ± 0.2	4.9 ± 0.1
89.5	2.757	4.4 ± 0.4	2.8 ± 0.3
83.0	2.807	3.6 ± 0.3	2.3 ± 0.2
73.3	2.886	2.7 ± 0.2	1.7 ± 0.1
57.8	3.021	2.5 ± 0.2	1.6 ± 0.1
45.2	3.141	2.8 ± 0.2	1.8 ± 0.1
34.1	3.254	3.6 ± 0.2	2.2 ± 0.1
23.5	3.370	5.1 ± 0.4	3.2 ± 0.3
12.0	3.506	8.1 ± 0.2	5.1 ± 0.1
2.8	3.623	12.7 ± 0.2	8.0 ± 0.1

Viscosity Data:

Temperature (°C)	$10^3/T$ (°K^{-1})	$\eta/T \times 10^3$ (centipoise °K^{-1})
86.1	2.78	6.95
73.5	2.88	8.56
60.3	3.00	11.0
49.4	3.10	13.8
38.4	3.21	17.9
24.5	3.36	28.4
0.0	3.66	84.0

Data for Indium Perchlorate Solution

Sample Composition: 2.04 gm $In(ClO_4)_3 \cdot 5H_2O$*

0.23 gm $Mn(ClO_4)_2 \cdot 2H_2O$

2.00 gm $H_2^{17}O$ enriched water

Relaxation Data:

Temperature (°C)	$10^3/T$ (°K^{-1})	$\frac{10^{-3}}{2\pi T_2}$ (Hz)	$\frac{10^{-4}}{T_2}$ (sec^{-1})
88.1	2.770	19 ± 3	12 ± 2
68.8	2.925	6.2 ± 0.3	3.9 ± 0.2
59.0	3.011	3.5 ± 0.1	2.2 ± 0.1
47.7	3.117	2.7 ± 0.1	1.7 ± 0.1
34.9	3.247	2.2 ± 0.1	1.4 ± 0.1
24.6	3.359	2.2 ± 0.1	1.4 ± 0.1
13.2	3.493	3.2 ± 0.1	2.0 ± 0.1
1.1	3.647	4.6 ± 0.1	2.9 ± 0.1
-5.1	3.731	8.2 ± 0.4	5.1 ± 0.3
-14.5	3.867	9.3 ± 0.3	5.9 ± 0.2

Viscosity Data:

Temperature (°C)	$10^3/T$ (°K^{-1})	$\eta/T \times 10^3$ (centipoise °K^{-1})
23.0	3.38	65.2
10.0	3.53	107
0.0	3.66	169
-4.7	3.73	213

*The solid was analyzed for indium only. It is believed that it was actually hydrolysed partially through heating in vacuum, as judged by comparison with the nmr data of Table I.

Data for Thorium Perchlorate Solution

Composition: 1.00 gm $Th(ClO_4)_4$

0.40 gm $Mn(ClO_4)_2 \cdot 2H_2O$

1.00 gm $H_2^{17}O$ enriched water

Relaxation Data:

Temperature (°C)	$10^3/T(°K^{-1})$	$\frac{10^{-3}}{2\pi T_2}$ (Hz)	$\frac{10^{-4}}{T_2}$ (sec^{-1})
29.5	3.305	2.3 ± 0.2	15 ± 1.5
23.8	3.368	9.1 ± 0.9	5.7 ± 0.6
19.0	3.423	7.4 ± 0.7	4.6 ± 0.5
15.6	3.464	3.0 ± 0.3	1.9 ± 0.2
11.0	3.520	3.9 ± 0.4	2.4 ± 0.2
9.1	3.540	3.2 ± 0.3	2.0 ± 0.2
3.0	3.62	3.9 ± 0.4	2.4 ± 0.2
-7.1	3.76	3.7 ± 0.4	2.3 ± 0.2
-10.3	3.81	4.2 ± 0.4	2.6 ± 0.3
-18.4	3.93	5.3 ± 0.5	3.3 ± 0.3
-21.8	3.98	7.5 ± 0.7	4.7 ± 0.5
-23.0	4.00	6.4 ± 0.6	4.0 ± 0.4

Viscosity Data:

Temperature (°C)	$10^3/T$ (°K^{-1})	$\eta/T \times 10^3$ (centipoise °K^{-1})
22.0	3.39	21.8
15.8	3.46	26.0
10.0	3.53	31.2
0.0	3.66	44.2
-9.1	3.79	63.7

Data for Figure 10

Ion	Ionic Radius (A)[1]	d (A)	$\frac{z}{d^3}\left(\frac{esu}{A^3}\right)$	log k_r (25°)
Al^{3+}	0.51	2.16	0.297	1.20 [2]
Be^{2+}	0.35	2.00	0.250	3.30 [2]
Ga^{3+}	0.62	2.27	0.256	3.11 [2]
Mg^{2+}	0.66	2.31	0.161	5.75 [2]
Cu^{2+}	0.72	2.37	0.150	9.9 [3]
Cr^{3+}	0.63	2.28	0.253	-5.3 [4]
Fe^{3+}	0.64	2.29	0.258	2.17 [5]
Fe^{2+}	0.74	2.39	0.146	5.6 [6]
Cr^{2+}	0.89	2.54	0.116	5.0 [7]
Ti^{3+}	0.76	2.41	0.214	6.0 [8]
Co^{2+}	0.72	2.37	0.150	6.0 [6]
Ni^{2+}	0.69	2.34	0.156	4.43 [6]
Mn^{2+}	0.80	2.45	0.136	7.5 [6]
Gd^{3+}	0.94	2.59	0.154	8.9 [9]
Rh^{3+}	0.68	2.33	0.237	-5.5 [10]

(1) Handbook of Chemistry and Physics, 47th Ed., R. C. Weast Ed.,

(Chemical Rubber Publishing Company, Cleveland, Ohio, 1966) p. F124

(2) This work

(3) C. W. Meredith, Lawrence Radiation Laboratory, UCRL-11704(1965)

(4) R. A. Plane and H. Taube, J. Amer. Chem. Soc., 56, 33(1952)

(5) M. R. Judkins, Lawrence Radiation Laboratory, UCRL-17561(1967)

(6) Ref. (3) of main Bibliography

(7) H. Charles, private communication; A. M. Chmelnick and D. Fiat,

J. Chem.Phys. 51, 4238(1969)

(8) Ref. (3) on main bibliography; A. M. Chmelnick and D. Fiat, J. Chem.

Phys. 47, 3986(1967)

(9) R. Marianelli, Lawrence Radiation Laboratory, UCRL-17069(1966)

(10) Ref. (2a) on main bib.